2016

Stability Sensitivity Of Low-Rise Steel-Moment Resisting Framed Buildings To Hazard-Independent Damage

Trey Reynolds Powell
University of Mississippi

STABILITY SENSITIVITY OF LOW-RISE STEEL-MOMENT FRAMED BUILDINGS TO HAZARD-INDEPENDENT DAMAGE

A Thesis
presented in partial fulfillment of requirements
for the degree of Master of Science in Engineering Science
in the Department of Civil Engineering

The University of Mississippi

by

Trey Reynolds Powell

May 2016

ABSTRACT

Structural stability has been the subject of much research in recent years. Simply, structural stability may be viewed as the ability of the structure's response to be relatively unaffected by perturbations to its system. Stability of low-rise steel-moment framed buildings and their sensitivity to perturbations from significant damage are the focus of this work.

Perturbations, or changes from the normal state of the structural system, have the ability to affect the structural response. Second-order geometric effects imposed through column axial loads, and/or initial out-of-plumbness during the construction process, are a common perturbation in steel framing systems. If the structural members subjected to these effects are damaged through a specific hazard, the effective stiffnesses of the members are reduced, and the consequence of the individual perturbations is amplified. Because such scenarios are feasible during the lifetime of a structure, robust methods to investigate structural stability sensitivity to damage and second-order geometric effects are desired.

A stiffness reduction factor is introduced into the analytical finite element formulation of a portal frame to account for hazard-independent damage. Second-order geometric effects are included in this formulation. This finite element formulation is created using Mathematica and its formulation is verified against idealized elastic critical buckling load theory. Next, the formulation is generalized to provide an ability to analyze the elastic buckling load of a wide range of portal frames. The finite element software, MASTAN2 and SAP2000 are utilized for verification purposes.

ABAQUS/CAE is chosen to further examine the stability of steel-moment frames. Several cases of gravity and lateral loads are applied to planar frame models. Again, the hazard-independent damage is introduced to the system in various cases and nonlinear geometric effects are accounted for. Results of this study suggest that the response is largely impacted by the amount and location of the hazard-independent damage, as well as the complexity of the frame system.

Lastly, the study is extended to a three-dimensional steel-frame system. The system is once again perturbed by several cases of nonlinear geometric effects and hazard-independent damage. Results of this study suggest that stability failure is a high concern in the cases considered.

DEDICATION PAGE

This thesis is dedicated to several special people in my life. To Christopher and Melanie Powell, without who's unwavering support, I would be lost. To my loyal best friend, Buzz, who despite hours of separation daily, always happily greeted me upon arrival. Lastly, to my late grandfather, Ira Wilbur Powell, whom I am certain was the true engineer in our family.

LIST OF ABBREVIATIONS AND SYMBOLS

(#)E Elastic Modulus Corresponding to Member (#)

(#)A Cross-Sectional Area Corresponding to Member (#)

(#)I Moment of Inertia Corresponding to Member (#)

(#)L Length Corresponding to Member (#)

α Hazard-Independent Damage Factor

P_{cr} Elastic Critical Buckling Load of Respective Model in Virgin Condition

$P_{\#}$ Vertical Load, (#) Indicates Chapter Specific Detail

$F_{\#}$ Lateral Load, (#) Indicates Chapter Specific Detail

M_p Plastic Moment

ACKNOWLEDGEMENTS

First and foremost, I would like to acknowledge Dr. Chris Mullen for his guidance and support throughout my graduate student career. Next, I would like to acknowledge Dean Alex Cheng for his support through a graduate fellowship and Professor Yacoub Najjar for his support through a teaching assistantship in the Department of Civil Engineering. Lastly, I would like to acknowledge my loving parents, Chris and Melanie Powell, for doing anything and everything they could do in order to provide for myself, as well as my sisters, Katie and Emily. Without the aforementioned parties, I would certainly not have completed this work.

TABLE OF CONTENTS

LIST OF FIGURES

LIST OF TABLES

1. INTRODUCTION

1.1 Objectives

The objective of this paper is to develop and implement a finite element modeling procedure using both analytical and computational methods to capture the sensitivity of steel-moment frame stability to second order geometric effects and hazard-independent damage. Analytical finite element expressions are first developed for steel portal frames in order to demonstrate competent use of the stiffness method. A computational model of a 4 story – 2 bay planar steel frame is then developed using ABAQUS/CAE. The effects of several hazard-independent damage scenarios on the stability of the steel frame are investigated. High magnitude lateral loads are introduced into the model to provide an additional perturbation, thereby amplifying the nonlinear geometric effects. Lastly, an ABAQUS/CAE computational model of a 3D low-rise steel moment frame system is developed and subjected to an identical analysis procedure. Conclusions regarding the stability of each model are stated and recommendations for future studies are suggested.

1.2 Motivations and Background

The safe and effective design of steel building structures considers a variety of limit states. Frequently, it is strength design that receives the most significant amount of consideration. To properly define strength design of steel structures, it is necessary first to quantify the specific applied loads to the corresponding structure or structural element. In doing so, it is possible to determine the causes and effects of the loads, or the load effect. In order to resist the load effect, the structural members must possess what is known as the required strength. The determination of steel structural members' sizes and their corresponding connections such that the strength of the structure is greater than the load effect is known as strength design (Geschwindner, 2008). Proper strength design minimizes the probability of undesirable yielding or rupture of critical structural members. While this is certainly an important aspect of structural design, consideration to other failure modes should be given. For instance, the investigation of structural system perturbations that have the potential to induce a critical imbalance in the structural response is imperative. It is this concept that is the premise of structural stability.

Stability, with respect to a structural system, may be viewed as the ability of the structure's response to be relatively unaffected by perturbations to the system. More simply, a change in the system in the form of damage, loading, initial displacements, etc. should not result in a disproportionate response, commonly in the form of large displacement. The lack of the ability of the structure's response to resist these perturbations leads to a system instability. Commonly, instability is illustrated through deflections that are not proportionate to the applied loads and is sensitive to even minor perturbations(Timoshenko & Gere, 1961).

To clearly understand the gradual development of instability at the structural system level, attention should be refocused to the structural response at the individual structural element level. When considering structural elements, instability may be defined as a condition wherein a compression member loses the ability to resist increasing loads and exhibits instead a decrease in load-carrying capacity. In more basic terms, instability occurs at the maximum point of a typical load – deflection curve (Galambos, 1998). At this maximum point, a phenomenon known as bifurcation of equilibrium occurs. Bifurcation of equilibrium is represented when the deformation of the element suddenly changes to a different pattern under an applied load. Often, this behavior is exhibited through an asymptotic relationship, where an infinitesimal increase in the applied load causes the deformation of the member to increase without bound. Figure 1.1 illustrates the bifurcation of equilibrium concept with a hypothetical load – deflection curve. Upon visualizing the occurrence of instability at the structural element level, it becomes necessary to investigate the mechanics that drive this specific response.

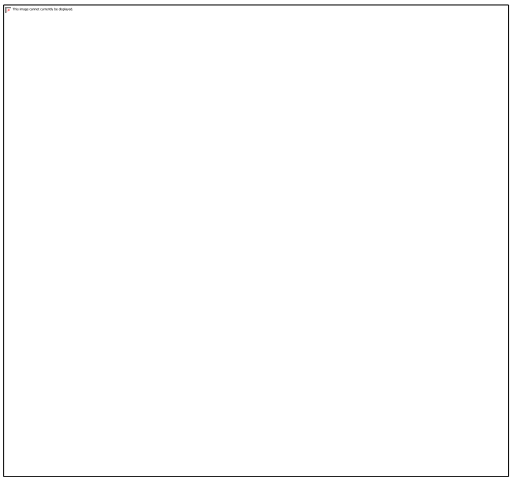

Figure 1.1 Equilibrium Bifurcation of Force vs. Deflection Curve

Compression members that exhibit bifurcation are frequently modeled in both analytical and computation analyses as beam – columns. Beam – columns are structural elements that have the ability to resist both axial and transverse loading. The bending moments that are caused from

such loadings are classified as two separate cases, primary and secondary bending moments. Primary bending moments are those that are imposed through the transverse loadings of the beam – column and/or applied or induced moments at its ends. The secondary bending moments are those that arise as a result of the axial force acting through the lateral displacement of the member. It is the latter that encompasses what is known as second – order, or nonlinear, geometric effects. Similarly to the bending moments, the nonlinear effects may be organized as two different cases, $P - \delta$ and $P - \Delta$ effects. $P - \delta$ effects are caused by the axial force acting through the lateral displacement of the member relative to its chord, whereas the $P - \Delta$ effects are caused by the axial force acting through the relative displacement of the two ends of the member (Chen & Lui, Stability Design of Steel Frames, 1991). Both the $P - \delta$ and $P - \Delta$ effects are illustrated by Figure 1.2. These second order effects are detrimental to compression members in that they may reduce the effective stiffness of the system. As the second – order geometric effects of the system increase, the lateral displacement increases, which in turn continues to amplify the nonlinear response. Simply, the lateral displacement of the beam – columns only leads to a further increase in lateral displacement. It is this behavior that produces the asymptotic relationship shown through the bifurcation of equilibrium displayed in Figure 1.1.

Figure 1.2 P – Δ & P – δ Second – Order Geometric Effects (RISA 2016)

The possibility of other detrimental effects to the stability of steel frame systems exists beyond those imparted through second – order geometric effects. Extreme loadings, such as earthquakes, blasts, hurricanes, etc. pose a real threat to the stability and stiffness of building structures. Various design provisions, including ASCE 7 and IBC, advocate for the consideration of these extreme loading events. However, these procedures often relate to the strength limit state of steel members. While adequate member sizes can be chosen to resist the extreme loads, inclusion of the damage to the structural members as a result of the event is often not considered in the design procedure. A possible explanation for the absence of this consideration is the associated labor intensive calculation and modeling of each specific damage scenario. Despite this fact, damage to structural systems through extreme loading is quite possible, and is documented by several notable agencies. For example, Figure 1.3 illustrates severe damage to a steel airport structure imparted by Hurricane Katrina and is recorded by the National Institute of Science and Technology (NIST).

Figure 1.3 Severe Damage – Frame Collapse Lakefront Airport New Orleans, LA (NIST 2006)

From scenarios such as Hurricane Katrina, a clear need to account for possible damage when investigating the stability of buildings structures is present. As an effort to avoid cumbersome calculations associated with particular damage events, this work attempts to provide

a hazard – independent approach for the application of damaged conditions. Regardless of the event that characterizes specific damage states, significant damage to structural members typically reduces the respective stiffness of the element. This principle is utilized in the hazard – independent damage approach by simply reducing targeted structural member's section moduli with respect to certain load directions and types. This procedure results in a weakened, or softened, structural system that may be used to approximate the damaged conditions imposed by a hazardous scenario. A simple cantilever beam and its response to a lateral load before and after the application of the hazard – independent damage procedure is shown in Figure 1.4.

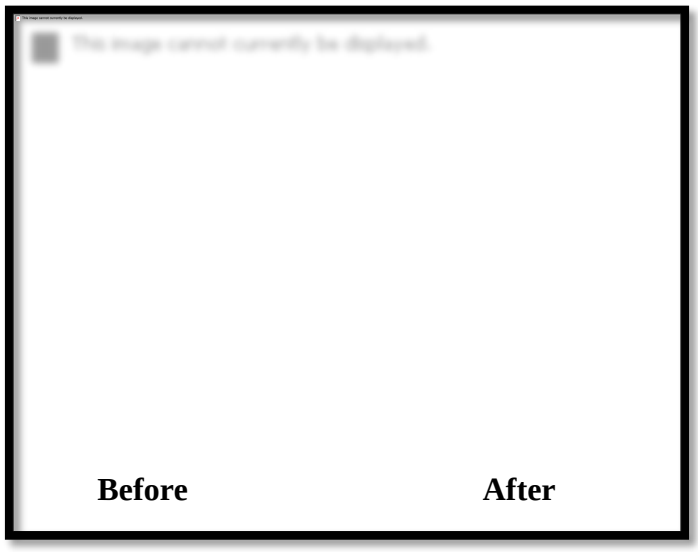

Figure 1.4 Effect of Hazard - Independent Damage Illustration

In the previous discussion, several contributions that may lead to the instability of a steel frame system have been outlined. Second – order geometric effects that are induced through axial loadings in beam – columns and/or initial out-of-plumbness during the construction process have significant impact on the stability of the structure. As the impact of these effects begins to grow due to lateral displacement, the phenomenon is, in turn, amplified. If hazard – independent damage is imparted to the structure, the effective stiffness is reduced, and again the second – order effects are magnified. Because the possibility of such a scenario occurring during a

structure's lifetime is possible, safe and effective design should incorporate the effects of nonlinear geometric effects and hazard – independent damage. Considering these perturbations for a single beam – column, it is possible to investigate how much of the structural response is controlled by including their effects. Figure 1.5 displays the contribution of both the elastic and geometric nonlinear response of a beam – column subjected to an axial load. It should be noted that only the diagonal terms of the stiffness matrix for this element were considered for this analysis. Further details associated with stiffness matrices are presented in Chapter 2.

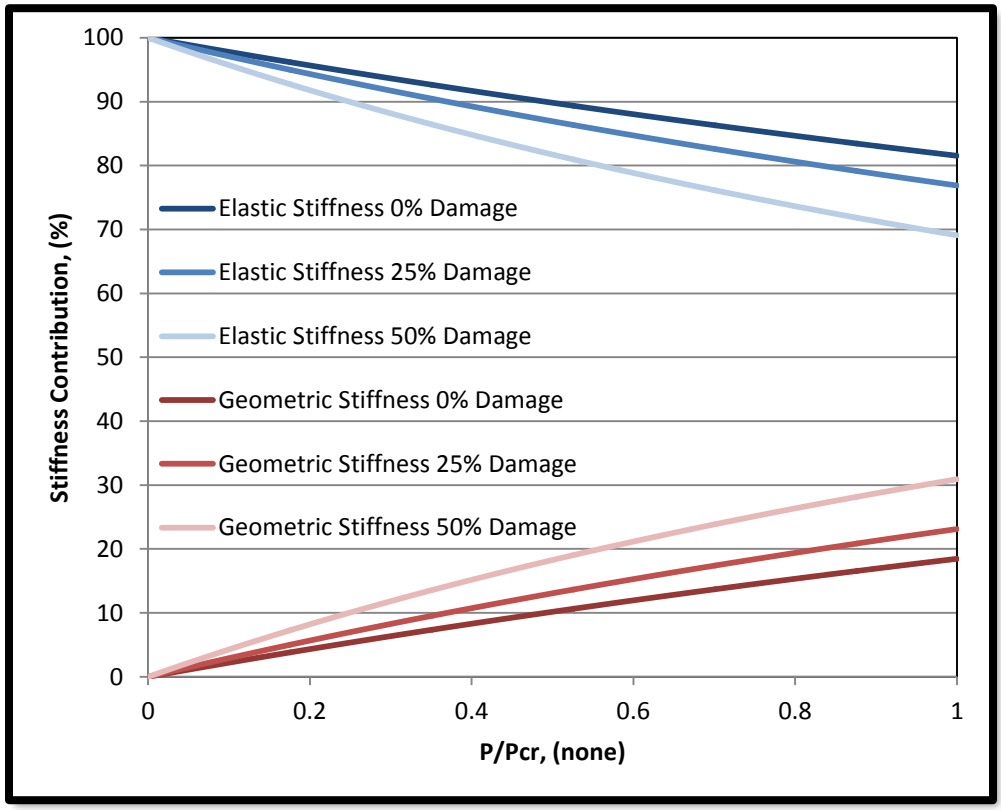

Figure 1.5 Contribution of Elastic & Geometric Responses for Diagonal Stiffness Matrix Terms for an Axially Loaded Beam – Column Element

Upon viewing Figure 1.5, several key principles can be concluded. As the axial load applied to the beam – column increases, the nonlinear geometric contribution of the response also increases. As the beam – column is weakened through hazard – independent damage, it is also clearly seen that second – order geometric contribution again increases. As the hazard –

independent damage continues to grow; a higher portion of the response will be governed by these perturbations. However, the effect of these factors on the stability of more complex and realistic steel frame structures is not as intuitive. The necessity for a robust finite element based procedure that captures the stability sensitivity to such perturbations is the motivation for this thesis.

1.3 Literature Review

Section 1.3 of this thesis is primarily concerned with the review of current literature. The specific works discussed in the following paragraphs were chosen based on their relation to the objectives and scope of research as defined in Chapter1.

In 2011, Balling and Lyon proposed the use of a single beam – column element per member to accurately complete second – order analysis of planar frames. Geometric nonlinearity was the main focus of their work. In order to achieve a high level of accuracy in their solution, the researchers utilized a corotational beam – column element. This finite element formulation refers to the idea that the local element frame continuously rotates with the element, and with respect to which, the standard, small-strain relationships can be applied (Balling & Lyon, 2011). This formulation is not utilized by most finite element software. Instead, the programs make use of total or Lagrangian formulations that involve numerical integration and interpolation functions. The reliability of the solution on such techniques produces a solution that is very much dependent on the number of elements that the frame member is divided into which the frame member is divided. In their work, Balling and Lyon illustrate the use of the corotational beam – column element achieves a solution that is comparable to that which is obtained through the finite element software, ABAQUS/CAE.

In an effort to provide sufficient theoretical background, Balling and Lyon detail the analytical development of the corotational beam – column element. It should be noted that the identical truncated geometric stiffness matrix utilized in this thesis is also found in their formulation. Upon successful derivation of the corotational beam – column element, several planar frame models are analyzed and the results are then compared to a number of ABAQUS/CAE with varying mesh refinement levels. The researchers were able to illustrate that

the corotational beam – column element leads to a displacement solution that is highly accurate. That is, a maximum percent error of 2% is reported. Through their research, Balling and Lyon show that a similar level of accuracy may only be found through a high level of mesh refinement in ABAQUS/CAE. For most of the cases investigated, this is around 25 elements per frame member.

Lastly, Balling and Lyon provide a plot that illustrates the percentage of the structural response that is controlled by both the elastic stiffness and geometric stiffness matrices for an example problem. Through this, it may be seen that the geometric stiffness matrix controls approximately 30% of the structural response. Their research helps to show the importance of accounting for second – order geometric effects. Similarly, because ABAQUS/CAE is utilized in this thesis, the refinement techniques illustrated by Balling and Lyon are considered for modeling purposes. Balling and Lyon's research provides motivation for investigating how the effect of damage could impact the second – order geometric stiffness contribution of a structure's response.

In 2015, Cortes, Liu, and Francisco completed a study that investigated the robustness of several steel framing strategies. To do so, the researchers modeled a 4-story steel framed building using SAP2000. The robustness of the structure was investigated by proposing several hypothetical 1st floor column removal cases. In essence, the ability of the structure to utilize alternate load paths in the event of a damage event is investigated. A typical load case is applied to the structure that includes dead, live, and notional loads. At the time of review, the results of a linear static analysis were available, while a nonlinear analysis was currently in the works. In their study, Cortes, Liu, and Francisco found that the case study building was fairly robust. That is, only a few structural members exceeded their design capacity under the column removal

scenarios, and stiffer members were suggested for their replacement. The work illustrated by the researchers helps to provide motivation for consideration of higher magnitude lateral loads. The notional loads used in their analysis may have been below a critical value that causes the second – order geometric effects to amplify, and therefore bring the stability of the structure into question. The critical lateral load value creating instability of the structure may provide valuable insight and additional robustness categorization. The researchers also discuss the effect of stiff stories on the stability of the structure; however this is not related to the studies found in this thesis.

In 2004, MacRae, Kimura, and Roeder provided a study concerning the effect of column stiffness on braced frame seismic behavior. While the work in the thesis is not necessarily related to seismic loadings and their effect, the 2004 study contains concepts that are important in generalized stability research. First, the researchers investigated the drift concentration factor as related to the number of stories the buildings contains. As one might expect, their research suggests that drift concentration is increased with the number of stories. This result is with respect to multistory buildings that have the same stiffness at each level. Similar to this investigation, the effect of column stiffness on the drift concentration at each floor is examined. The researchers provide a result that suggests that as the column stiffness ratio is increased, the drift concentration is reduced. Inversely, as the column stiffness ratio is decreased, the drift concentration at this specific floor is increased. The column stiffness ratio can be seen as a very closely related concept to the hazard – independent damage variable provided in this thesis. The research provided by MacRae, Kimura, and Roeder motivates a broader scope of investigation. That is, the reduction of beam, as well as column stiffnesses may be examined. Also, the reduction of stiffness on several floors, as opposed to a single floor, may provide insight into a

critical weakened state of the structure. The hazard – independent damage application attempts to address this consideration.

Another work related to seismic loadings and structural responses was reviewed for this thesis. This work was entitled "Collapse Fragility of Steel Structures Subjected to Earthquake Mainshock-Aftershock Sequences," and was completed by Li, Song, and Van De Lindt. In their work, it is stated that the P-Delta effects, strength, and stiffness degradation of components and loading history mainly contribute to the degradation of structural collapse capacity (Li, Song, & Van De Lindt, 2014). Various trends are plotted showing this phenomenon. The most important concept in their work as it relates to this thesis is loss of stability after a damage event, and how the perturbed system now responds to loadings. When subjected to a mainshock earthquake only, it may be seen that instability or collapse is not a high concern. However, as the structure is subjected to aftershock following the mainshock, a large decrease in the collapse resistance of the structure is seen. This idea motivates the investigation of how a structure's response is changed after a damage event. Consideration should be given to the remaining capacity of the structure after the damage event. Examining the possibility of collapse under non-severe loadings following a damage event could provide a more descriptive stability analysis of structures.

The final work reviewed for this thesis was entitled "Collapse Analysis and Testing of an Existing Building," and was presented by Sezen and Akah in 2015. In their work, an existing four – story steel building is instrumented and physically tested by removing one of the first – story columns from the perimeter frame. SAP2000 is utilized by the researchers to create preliminary planar frame models and their results are compared to the field data. The planar frame models drastically exceed the field results. As stated in their work, this is mainly due to

the fact that load redistributions are not considered in the 2-D model (Sezen & Akah, 2015). The researchers believe including nonlinear effects in the modeling procedure will help to improve the solution of the planar frames. The main motivation derived from this work is related to the column removal procedure exercised in the field. While this may have provided an easier procedure, it is difficult to imagine a damage scenario in which only a single column is completely destroyed, and effects to other structural members are not found. The building in the field study does not collapse, however the reader is left to determine what may have happened as a result of distributed damage. This thesis aims to suggest damage scenarios in which stiffness loss occurs in several elements. This provides a scenario that is much more feasible than that of a column removal scenario. The following section provides the scope of research associated with this thesis.

1.4 Scope of Research

The first chapter of this thesis is the Introduction and covers the Objectives and Motivations of the research. Core concepts that influence the stability of steel framed buildings are defined therein. Specifically, second – order geometric effects and hazard – independent damage are both described and their importance in the following analyses is stated. The scope of these concepts in practical situations is now summarized.

Chapter 2 first discusses the theory of finite element analysis of planar frames and its corresponding analytical development beginning with the formulation of both the linear elastic and nonlinear geometric stiffness matrices of a beam – column element. Following this procedure, a group of three beam – column elements are assembled in a portal frame configuration and the global stiffness matrix containing these elements is derived. It should be noted that a multiplicative hazard – independent damage term, α, is introduced in the bending resistance terms of the left column. An effort is made to ensure the proper understanding and application of both the nonlinear geometric effects and the α term. To do so, the analytical finite element assembly of the portal frame is programmed in Wolfram Mathematica and elastic critical buckling load analyses are performed. Identical assumptions to those made in a referenced theoretical result regarding the section properties of the portal frame members are made in the Wolfram Mathematica script. Upon verification of the elastic critical buckling load result, the script is then generalized so as to provide an ability to determine the critical buckling load of any fixed – base portal frame. As a final step in this analysis, α is utilized to account for scenarios in which the bending resistance of the left column is limited to fractions of its virgin capacity. Again, elastic critical buckling load analyses are performed and the effect of the hazard – independent damage on the buckling load is noted.

Lastly, the finite element software, MASTAN2 and SAP2000 are chosen to verify the accuracy of the Wolfram Mathematica script.

Chapter 2 concludes with the development of several computational models of steel portal frames using ABAQUS/CAE(ABAQUS Inc., 2003). The models are organized by two distinct loading cases. The first loading case investigated is defined by an initial, and constant, lateral load. The analysis then proceeds with a linearly increasing vertical load. Inversely, the second loading case investigated is defined by an initial, and constant, vertical load. The analysis is then continued with a linearly increasing lateral load. Each loading case includes analyses of the virgin condition, and several hazard – independent damage scenarios affecting the left column. Finally, system stiffness curves are developed and conclusions regarding the stability of the portal frame are presented.

In Chapter 3 of this work, the analyses performed with the portal frames are extended to a more realistic steel frame structure. ABAQUS/CAE is again utilized to develop a computational finite element model of a 4 story – 2 bay planar steel frame. Unlike in Chapter 2, only a single loading case is investigated. This loading case is described by an initial, and constant, vertical load. The analysis is then continued with the application of a linearly increasing lateral load. This load case was chosen because it is representative of a condition that is more common in building structures. This condition is defined as a gravity load that is always present and the probability of a lateral load being generated by an extreme load. Three separate hazard – independent scenarios are investigated under the application of this load case. The first damage scenario effectively damages only the left exterior column of the second floor of the frame. The second damage scenario effectively damages only the interior column of the second floor of the frame. The third and final damage scenario imposes damage to all three columns of the second

floor of the frame. It should be noted that the three damage cases chosen were selected based on a "system" elastic buckling load of the frame. To conclude this chapter, several figures related to the stiffness and stability of the planar frame are constructed and remarks are made concerning their results.

Chapter 4 presents a computational model of a 3D steel frame system developed using ABAQUS/CAE. Once again, the loading case of an initial, and constant, vertical load followed by a linearly increasing lateral load is investigated. Similar to Chapter 3, three separate damage scenarios are investigated. The first scenario applies damage to all columns of the second floor. The second scenario applies damage to several interior structural elements, creating a case that is similar to an interior blast event. The final scenario applies damage to several exterior structural elements along a single face of the frame structure, similar to an extreme wind event. Chapter 4 concludes with the demonstration of the sensitivity of the system's stability and stiffness to perturbations through results presented in a number of figures.

Lastly, Chapter 5 presents conclusions that summarize key results from the various computational simulations performed in earlier chapters. Recommendations for future studies concerning the stability of steel frames subjected to damage scenarios are made. Lastly, it should be noted that the analyses performed within this work do not include the effects of material nonlinearity. Calculations are shown verifying that the range of structural response under investigation does not contain significant plasticity of the structural members in the steel frame system. All results of this study are subject to imposed assumptions, constraints, etc. and should not be taken out of this context without consideration of their effects.

2. ANALYTICAL FEA OF STEEL PORTAL FRAMES

2.1 Portal Frame: FEA Theory Verification

To begin the investigation of the stability of steel frame systems, an analytical finite element model of a simple portal frame is developed. The objective of this analysis is to provide a theoretical background of second – order geometric effects and hazard – independent damage in an effort to ensure accurate application in the following chapters.

Before assembling the full portal frame system, it is necessary to obtain the elastic stiffness matrix corresponding to a single beam – column element(Hughes, 1987). This matrix is derived utilizing elementary mechanics theory and hermite shape functions. A typical beam – column element and its corresponding elastic stiffness matrix is illustrated in Figure 2.1.1.

Figure 2.1.1 Beam - Column DOF Orientation & Elastic Stiffness Matrix

It is necessary to note that degrees of freedom 1 and 4 correspond to the axial deformation of the beam – column and its terms are accounted for by columns 1 and 4 of the elastic stiffness matrix. Similarly, degrees of freedom 2 and 5 correspond to bending deformation under the action of end shear forces of the beam – column and its terms are accounted for by columns 2 and 5. Finally, degrees of freedom 3 and 6 correspond to bending deformation under the action of end rotations of the beam – column and its terms are accounted for by columns 3 and 6. In Figure 2.1.1, the prefix "C1" is used to distinguish terms that are associated with column 1, or the left column, of the portal frame. This distinction becomes vital during the assembly of the global stiffness matrix. The terms "E," "A," "I," and "L" define the elastic modulus, cross – sectional area, moment of inertia (second moment of area), and length of the beam – column element, respectively. In this analysis, the hazard – independent damage term, "α," is applied to only the bending resistance terms of column 1 of the portal frame. This application is illustrated by the terms with red underlines in Figure 2.1.1. When "α" is equivalent to 1, the beam – column does not have any damage applied to its bending resistance. Alternatively, "α" holds a value of 0 when the beam – column is subjected to maximum damage. That is, the terms including "α" are reduced to null values, and the terms no longer contribute stiffness to the element. Only the bending resistance of column 1 was chosen to be damaged so as to not affect the member's axial capacity. Limiting the axial capacity of the beam – column would cause disastrous effects to the simple portal frame system because it does not possess a significant number of alternate load paths.

Upon completing the derivation of the elastic stiffness matrix of a beam – column element, the nonlinear geometric stiffness matrix is considered. As stated in previous discussion, the nonlinear geometric stiffness matrix arises from the $P - \Delta$ and $P - \delta$ effects. The dependence

of these terms on the axial load carried in the beam – column element leads to the nonlinear effect on the deformation of the element. Figure 2.1.2 illustrates the P – Δ and P – δ effects of the beam – column element and the additional shear and moment deformations introduced through the nonlinear geometric stiffness matrix(McGuire, Gallagher, & Ziemian, 2000).

Figure 2.1.2 P- Δ & P - δ Effects of a Beam –Column Element & Resulting Nonlinear Geometric Stiffness Matrix

It can easily be seen that the axial load carried by the beam – column element is the primary factor driving the magnitude of the geometric stiffness matrix. As this axial load is increased, the beam – column begins to buckle and displace laterally. Therefore, as the magnitude of the axial load increases, the effects of the nonlinear geometric stiffness matrix also increase. More simply, lateral displacement of the element only gives way to more lateral displacement. Columns 2 and 5 include the terms that contribute additional shear forces in the beam – column element while columns 3 and 6 include terms that contribute additional bending moments in the beam. Again, the prefix "C1" appears to distinguish the axial load, "P," that is carried by column 1, or the left column of the portal frame. Note that the sign of each term depends on the direction of "P," where a negative value indicates compression and positive value indicates tension. Lastly, it should be clarified that the nonlinear geometric stiffness matrix utilized by this derivation is truncated. The stability functions used to derive the matrix are

simply expanded and the higher order terms are neglected(McGuire, Gallagher, & Ziemian, 2000). The accuracy of this approximation was determined to be sufficient while investigating elastic critical buckling loads.

The analytical derivation detailed in the previous paragraphs is repeated for the remaining two elements of the portal frame. The two elements are "C2" and "B1." The abbreviation "C2" corresponds to column 2, or the right column of the portal frame. Similarly, the abbreviation "B1" is associated with the single beam connecting the two columns of the portal frame. The elastic stiffness and nonlinear geometric stiffness matrices for the remaining elements continue identically to the procedure utilized for column 1. The matrices of column 2 will be identical to those seen for column 1; however a significant difference arises for the beam. The beam is not allowed to carry an axial load, which assigns a value of 0 to "P," and therefore the nonlinear geometric stiffness is effectively eliminated for this element. Once this process is completed, the 3 beam – column elements are now ready to be assembled to construct the portal frame.

For proper assembly of the portal frame system, the degrees of freedom of each element must be oriented properly. This process is completed through the appropriate use of transformation matrices(Hughes, 1987). This procedure is typical of analytical finite element formulations and is not extensively described within this work. The computational software Wolfram Mathematica is utilized for this assembly process. After each beam – column element is transformed to its proper orientation, the global stiffness matrix is then formed. The resulting global stiffness matrix is of the size 12 x 12. This result includes the application of the hazard – independent damage term to column 1, and the second – order geometric effects of both columns 1 and 2. Figure 2.1.3 displays the global stiffness matrix of the portal frame prior to imposing boundary conditions.

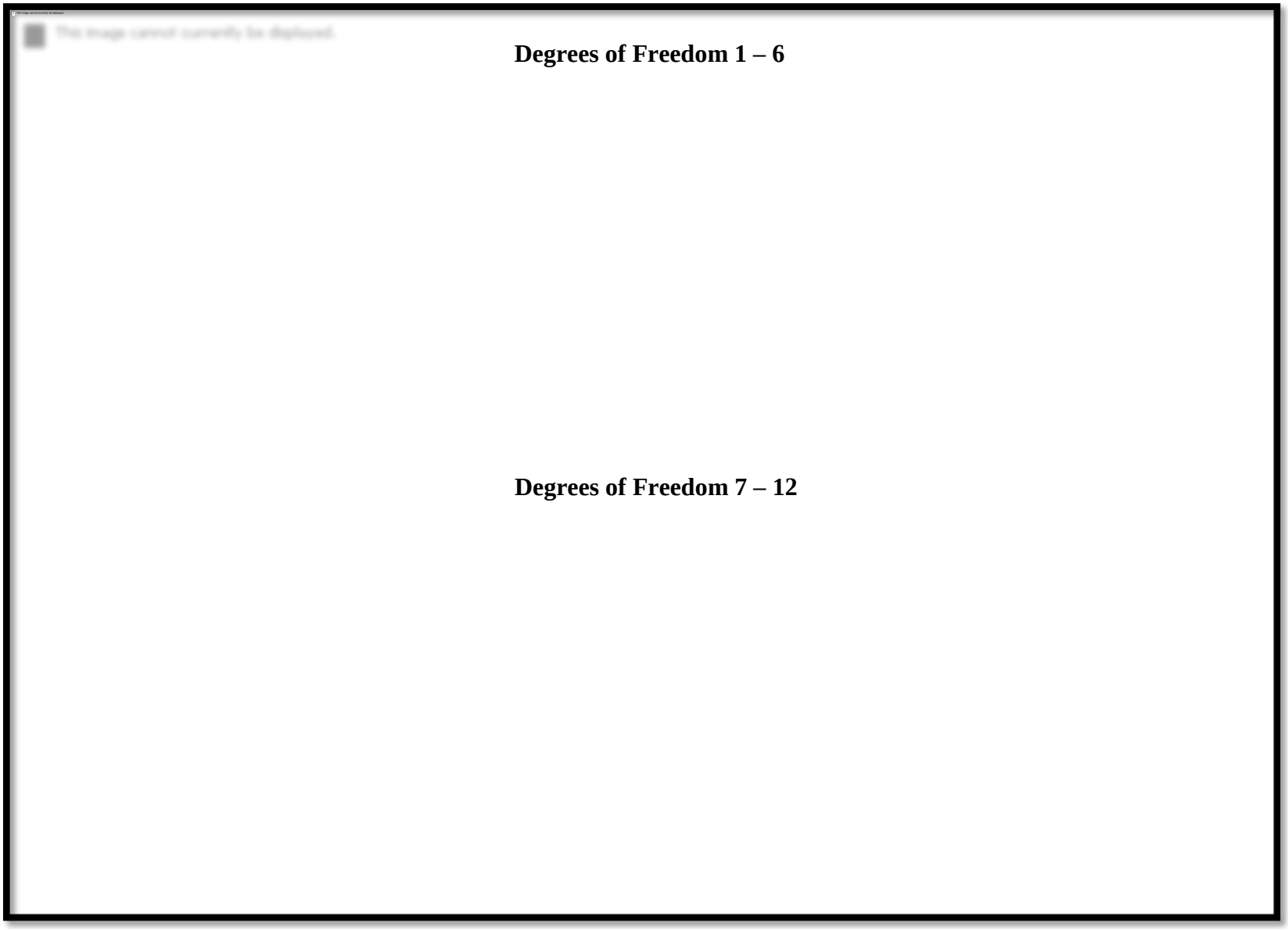

Figure 2.1.3 Portal Frame Global Stiffness Matrix

To verify that the portal frame analytical formulation is correct and the second – order geometric effects and hazard – independent damage are properly applied, elastic critical buckling load analysis is performed. The buckling load case investigated is described by vertical point loads at the top of the two columns. As previously defined, these axial loads induce the second – order geometric effects resulting in column buckling. If the global stiffness matrix and its corresponding terms are derived correctly, the result of the buckling load analysis can be verified using an acceptable source of theory(Chen & Lui, Structural Stability Theory and Implementation, 1987). In their work, the analytical finite element method is utilized to determine the elastic critical buckling load of a pin based portal frame that is permitted to sway. Unlike the methods used to produce the global stiffness matrix shown in Figure 2.1.3, several simplifying assumptions are made in the selected text. First, the lengths of all three elements in the portal frame are assumed to be equivalent. In doing this, a point of symmetry about the midpoint of the beam is created. Because of this, only half of the portal frame assembly is necessary for the analysis. Secondly, the section properties of all three members in the portal frame assembly are assumed to be identical. This allows for further simplification and factoring of similar terms in the global stiffness matrix. The resulting global stiffness matrix is reduced to a size of 4 x 4 using the simplifying assumptions. The original portal frame configuration, the simplified portal frame configuration, and the resulting global stiffness matrix obtained by Chen & Liu is shown by Figure 2.1.4.

Figure 2.1.4 Pin Based Portal Frame with Chen & Liu Reduced System & Reduced Global Stiffness Matrix (Chen & Liu, 1987)

The elastic critical buckling load analysis is conducted with the use of the simplified system. To evaluate the critical load, the determinant of the global stiffness matrix is first calculated. Next, the equation obtained from the determinant is equated to zero. In doing so, the equation now represents the bifurcation of equilibrium condition of the portal frame. That is, the system stiffness of the portal frame is now of null value, and displacement begins to increase without bound under the critical axial load, "$P_{cr.}$" Simply, the buckling phenomenon has occurred in the portal frame. To determine the elastic critical buckling load, the variable "P" is solved for in the determinate equation that has been equated zero. Through the simplifying assumptions, Chen & Liu's resulting value of "P_{cr}" may be left in terms of the section properties of the elements, as shown in Figure 2.1.4. However, the generalized global stiffness matrix shown in Figure 2.1.3 provides a result that is much more cumbersome. The elastic critical buckling load may only be determined by first assigning values to all three element's section properties. As a final step, a W10 x 68 steel section is chosen for each member and its corresponding section properties are substituted into both expressions for the elastic critical

buckling load. The section properties of a W10 x 68 steel section and the elastic critical buckling obtained from both methods are shown in Table 2.1.1. Appendix A provides the calculations completed using Wolfram Mathematica for the pin based portal frame.

Table 2.1.1 W10 x 68 Section Properties & Symmetric Pin Base Portal Frame Elastic Critical Buckling Load Comparison

W10 x 68			
A	**I**	**E**	**L**
in^2	**in^4**	**ksi**	**in**
19.9	394	29000	144

P_{cr}		
Mathematica	**Chen & Liu**	**Percent Difference**
kips	**kips**	**-**
1006.43	1008.37	0.19

Examining the results of the elastic critical buckling load analyses using both the generalized and simplified global stiffness matrices, several conclusions can be made. Because there is less than 1% difference between the two calculated values of "P_{cr}", it can be assumed that the analytical formulation of the portal frame is correct. Also, it can be assumed that the nonlinear geometric stiffness matrices are applied correctly. Finally, the effective use of the hazard – independent damage term may also be assumed. By setting this term equivalent to 1, the undamaged case evaluated by Chen & Liu is replicated with the generalized global stiffness matrix using Wolfram Mathematica. It should be noted that the slight difference between the values of "P_{cr}" may be attributed to the axial deformation of the beam – column elements. The analysis completed by Chen & Liu does not allow for extensible/compressible members, while the formulation with the generalized global stiffness matrix includes this behavior. Upon verifying the analytical finite element model of the portal frame, the elastic critical buckling load analysis is extended in the following section.

2.2 Elastic Buckling Load Analysis of Fixed Base Portal Frame: FEA Comparison

The elastic critical buckling load analysis of a portal frame is extended in this section. In this study, the portal frame is now fixed base, as opposed to the previous study wherein the portal frame is pin based. The hazard – independent damage term is included for several different values and its effect on the value of "P_{cr}" is determined.

The analytical finite element analysis of the portal frame begins identically to that outlined in Section 2.1 of this work. A difference arises from the imposed boundary conditions. Because the portal frame is now supported through fixed bases, six degrees of freedom are now restrained. The restrained degrees of freedom allow the elimination of rows and columns 1, 2, 3, 10, 11, and 12 in the generalized global stiffness matrix presented in Figure 2.1.3.

Upon imposing the fixed base boundary conditions, the elastic critical buckling load analysis is again completed by setting the determinate of the global stiffness matrix equal to zero and solving for "P." This analysis is performed for several cases of hazard – independent damage, ranging from 0% to 90% damage. Again, "α" is applied only to the bending resistance terms of column 1, or the left column.

Similar to the validation provided in the previous section, two computational finite element software programs were utilized for verifying the elastic critical buckling load of the fixed base portal frame obtained with the analytical finite element model. These programs are SAP2000 and MASTAN2. Both programs posses a buckling analysis in which only the critical buckling load is obtained, as opposed to reactions, displacements, and etc. This buckling function was determined to be appropriate for the analyses performed in this section. Within the two computational finite element programs, the hazard – independent damage was imparted to column 1 through the use of modification factors. For this instance, the modification factors for

the moment of inertia of column 1 in both SAP2000 and MASTAN2 is equivalent to the hazard – independent damage term, "α," developed in the previous section.

Unlike the investigation performed in Section 2.1, the fixed base portal frame is allowed to contain different section assignments for columns 1 and 2, and the connecting beam. For the ability to obtain a more realistic critical buckling load, a typical assembly where the beam is a stiffer section than the column sections is chosen. Specifically, the columns are assigned to be W10 x 68 steel sections, and the beam is assigned to be a W18 x 40 steel section. The lengths of the columns and beam were allowed to be 144 inches and 300 inches, respectively. Upon creating the fixed base portal frame in both the analytical and computational models, the elastic critical buckling load analysis was performed. It should be noted that the calculations performed by Wolfram Mathematica for the analytical model can be found in Appendix B. Figure 2.2.1 depicts both the original configuration and deformed configuration of the fixed base portal frame. Column 1, or the left column of the portal frame, is circled in red so as to identify it as the member receiving damage.

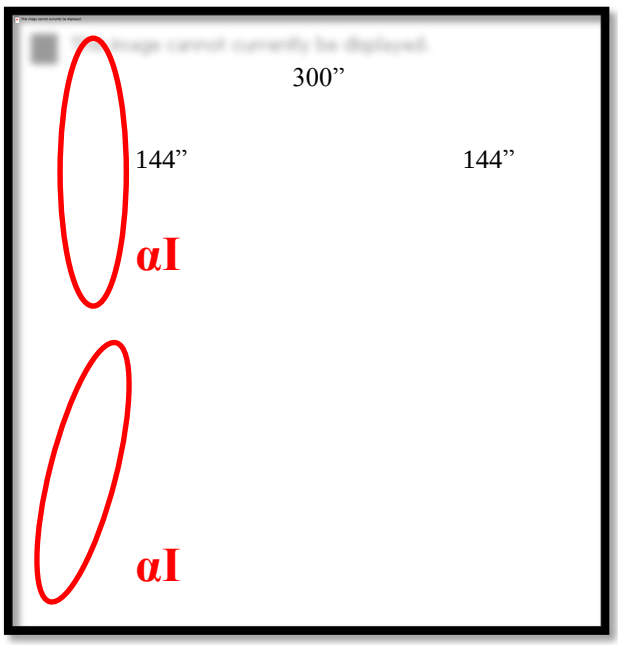

Figure 2.2.1 Original & Deformed Configuration of Fixed Base Portal Frame

The elastic critical buckling loads of the fixed base portal frame are obtained with respect to several hazard – independent damage values imparted to column 1. The values of the hazard – independent damage, α, are started at 1 and are decreased by increments of 0.1 to a minimum value of 0.1. Again, it should be noted that when α is equated to 1, the virgin condition is present, whereas when α is equated to 0, the member absorbs complete damage and its stiffness is of null value. The elastic critical buckling loads obtained through the analytical finite element model, as well as the two computational finite element models, are displayed for each damage case in Table 2.2.1. Also shown, is the percent difference between the calculated values of the elastic critical buckling load obtained through each method.

Table 1.2.1 Elastic Critical Buckling Loads of Fixed Base Portal Frame with Various Hazard - Independent Damage Levels of Column 1

Damage Factor	Mathematica	MASTAN2	SAP2000	Mathematica	MASTAN2	SAP2000
*α**	*Pcr*	*Pcr*	*Pcr*	*% Difference*	*% Difference*	*% Difference*
-	*kips*	*kips*	*kips*	-	-	-
1	3792	3792	3792	-	0.0003	0.0005
0.9	3651	3651	3651	-	0.0003	0.0005
0.8	3501	3501	3501	-	0.0000	0.0006
0.7	3337	3337	3337	-	0.0000	0.0005
0.6	3157	3157	3157	-	0.0000	0.0004
0.5	2956	2956	2956	-	0.0003	0.0003
0.4	2729	2729	2729	-	0.0000	0.0004
0.3	2469	2469	2469	-	0.0000	0.0002
0.2	2165	2165	2165	-	0.0000	0.0004
0.1	1804	1804	1804	-	0.0000	0.0002

*α = 1 Denotes Virgin State; α = 0 Complete Damage/Section Loss

Several concluding remarks can be made concerning the results presented in Table 2.2.1. First, it can be seen that the percent difference between the values of "P_{cr}" obtained using the analytical formulation and the computational finite element programs is insignificant. With a

maximum value of 0.0006, the percent difference found between the elastic critical buckling loads can likely be attributed to rounding approximations. From this, a clear understanding, and application of, both the second – order geometric effects and hazard – independent damage term is illustrated. It can also be seen that the value of "P_{cr}" is reduced as damage to column 1 is increased. The damage increase to column 1 is carried out through a decrease in "α." While its effect does not seem devastating to the fixed base portal frame until high values are imposed, it is important to remember that the hazard – independent damage is affecting only the bending resistance of column 1. If the term was applied to the axial resistance of this member as well, a much more significant impact to the stiffness and stability of the portal frame would be found. Although the change in the elastic buckling load is not greatly decreased at low damage levels, it is evident that the hazard – independent damage is an important parameter in the structural response. It is expected that as the system becomes more complex and the hazard – independent damage is distributed throughout the frame system, its effect will no longer be subtle.

2.3 Stability Sensitivity to Hazard-Independent Damage of Fixed Base Portal Frame

The objective of the study performed in this section is to extend beyond an elastic critical buckling load analysis. The fixed base portal frame described in the previous sections is again utilized. For the geometry and section assignments of the portal frame, please refer to Figure 2.2.1. The response of the frame system to several load cases related to the previously obtained elastic critical buckling load is examined. Specifically, the changes in the portal frame's stiffness due to hazard – independent damage and second – order geometric effects are determined. The stability of the portal frame system is also inferred through this result. The computational finite element software ABAQUS/CAE is utilized for all models presented in this section.

To begin the stiffness/stability analysis of the portal frame assembly, load cases must first be defined. The first load case considered is defined by an initial, and constant lateral load, followed by a linearly increasing vertical load. Both the lateral and vertical loads are treated as point forces. While the vertical loads are applied to the top joints of columns 1 and 2, the lateral load is applied only to the top joint of column 1. This load case will hereafter be referred to as Load Case #1.

The vertical load begins at a value of 0 and is linearly increased to a maximum value of 3530 kips, the virgin state elastic critical buckling load of the portal frame. It should be noted that this value is slightly less than that shown in Table 2.2.1 as a result of ABAQUS/CAE including the effects of shear area.

Several different values are assigned to the constant initial lateral load in this load case. The first value is 0.5 kips. This value was chosen simply as a system perturbation. Without this load, ABAQUS/CAE is unable to capture second – order geometric effects. A lateral load of

small magnitude must be present in order for the buckling phenomenon to be captured by this software. In the absence of a lateral load, the portal frame is simply compressed, an idealization that is common to computation finite element programs. The second value of the lateral load is that of a notional load. As defined by the American Institute of Steel Construction, a notional load is 0.2% of the total gravity load with respect to floor level. This calculated value is applied as a lateral load at the respective floor level. The goal of the notional load is to account for initial "out-of-plumbness" and other imperfections that may induce second – order geometric effects. Because the gravity load is linearly increasing for the case of the portal frame, it is not possible to obtain 0.2% of the gravity load at a constant value. For this reason, an approximation is made; 0.2% of half of the maximum gravity load applied to the portal frame is chosen. The calculation is simply 3530 kips per column, applied at two columns, giving a total gravity load of 7060 kips. Dividing this maximum value by 2, gives 3530 kips, 0.2% of which leads to a notional load of 7.06 kips. The last value given to the lateral load is that of 3 times the previously calculated notional load. This value was chosen as a "worst case" scenario, describing severe "out-of-plumbness" or other imperfections.

After defining Load Case #1, hazard – independent damage scenarios are selected to complete the portal frame stiffness/stability computational model. Similar to Section 2.2, damage is imparted to column 1, or the left column, only. The virgin, 10%, 20%, and 30% damage conditions are imposed on column 1 and the respective analyses are performed. It should be noted that the hazard – independent damage term, "α," is again applied only to the bending resistance of column 1. However, ABAQUS/CAE does not possess the modification terms of the section properties as seen in SAP2000 and MASTAN2. To apply the hazard – independent damage in ABAQUS/CAE, the reduced moment of inertia, or "αI," is first

calculated. Next, the cross – section dimensions of an idealized W shape yielding the value of "αI" are chosen. It is determined that the application of the hazard – independent damage using this method is sufficiently accurate for the analyses performed within this section.

Figure 2.3.1 is provided as a summary of the concepts related to Load Case #1. The variable "P" indicates the linearly increasing value of the vertical load. The initial and constant lateral load is indicated by the variable "F_0." Lastly, the red circle surrounding column 1 illustrates the member receiving the hazard – independent damage. Again, for the geometry and section assignments of the fixed base portal frame, please see Figure 2.2.1.

Figure 2.3.1 Load Case #1 & Hazard - Independent Damage Application

The computational finite element models considering the details associated with Load Case #1 are processed. Before presenting the results, several post – processing details should be made clear. First, because the lateral load applied for Load Case #1 is constant, it is not considered as a primary variable to be assigned an axis in the following figure. Rather, the linearly increasing vertical load is tracked and is noted as a primary variable. To provide a more intuitive reference of its magnitude, the vertical load is normalized by the virgin state elastic

critical buckling load. This provides a minimum and maximum value of 0% and 100%, respectively. Next, in order to provide a common system stiffness curve, the displacement corresponding to the applied load must be obtained. For this instance, the lateral displacement of the portal frame under the constant lateral load and linearly increasing vertical load is tracked. Again, to illustrate an intuitive result, the lateral displacement of the portal frame is normalized by the column height, 144". The maximum boundary value of the lateral displacement is allowed to be 0.1% of the column height. This is a "worst case" limitation imposed by the structural design specifications of the American Society of Civil Engineers. The condition is characterized as a building that is an essential facility, the failure of which would present detrimental effects to emergency response agencies and/or significant economic loss. Lastly, it should be noted that the deformed configuration of the portal frame under each load scenario defined in Load Case #1 is presented at a scale factor of 1. That is, the deformed configuration is not amplified and represents the deformed shape expected due to the applied loads. Figure 2.3.2 provides the stiffness/stability results of the portal frame with hazard – independent damage applied to the left column and subjected to the applied loads as defined in Load Case #1. The identifiers A, B, C, and D define the virgin state, 10% damage, 20% damage, and 30% damage cases, respectively.

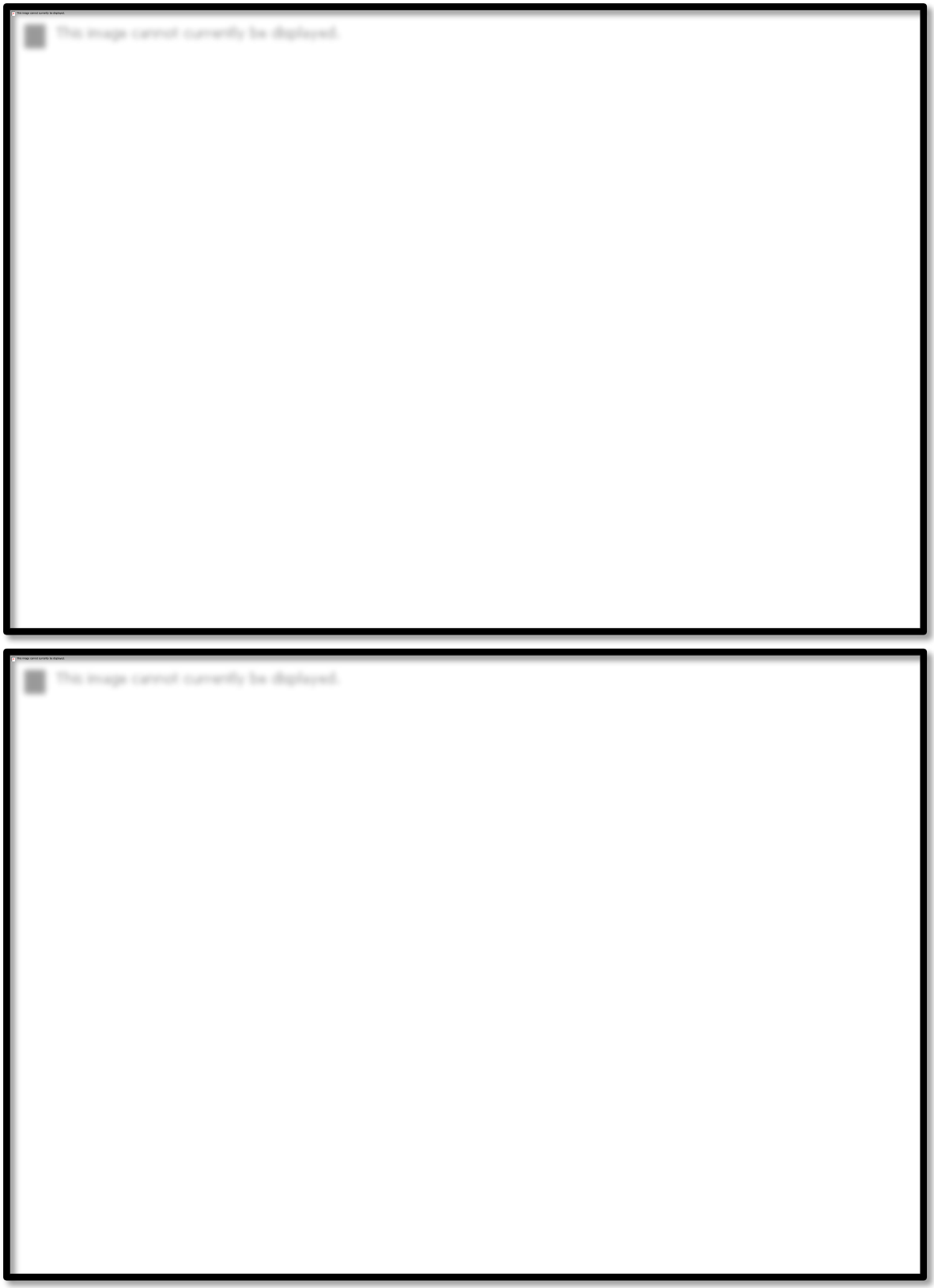

Figure 2.3.2 Stiffness Curves Due to Load Case #1: (A) Virgin State (B) 10% Damage (C) 20% Damage (D) 30% Damage

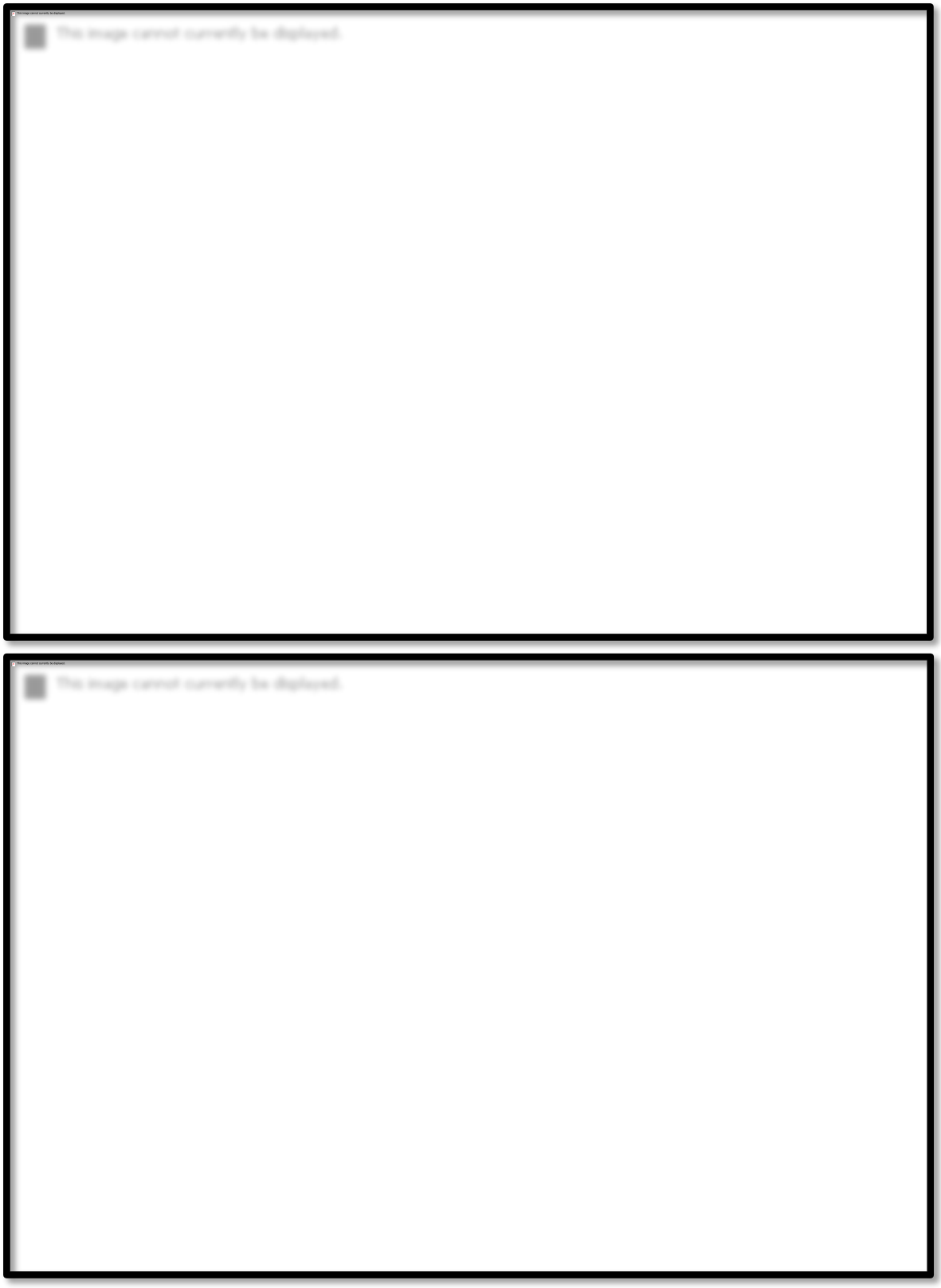

Figure 2.3.2 Stiffness Curves Due to Load Case #1: (A) Virgin State (B) 10% Damage (C) 20% Damage (D) 30% Damage

Attention is first focused on the virgin state stiffness curve shown in Figure 2.3.2 (A). The bifurcation of equilibrium concept is clearly illustrated by the 0.5 kip lateral load curve. The slope of this curve is reasonably constant until the vertical load is increased to a value of approximately 80% of the elastic critical buckling load. At this location, the slope begins to decrease quite rapidly and an asymptotic behavior is displayed. The slope of this curve directly relates to the stiffness of the fixed base portal frame. Noting this, it can easily be inferred that the frame assembly's stiffness is stable to a value of approximately 80% of the elastic critical buckling load. At this value, the stiffness begins to change as a result of the second – order geometric effects. As the lateral displacement increases from these effects, the nonlinear effect is amplified, and it may be stated that the fixed base portal frame has reached a point of instability. In simple terms, a small increase in the applied loads results in a disproportionate increase in the lateral displacement. It should be noted that this curve represents an ideal case where a negligible lateral load is applied and the response is controlled primarily by the axial load received by the columns. For this reason, the system exhibits a null stiffness value at exactly the elastic critical buckling load. A large difference in the portal frame's response is seen when the lateral load is increased to the notional value. The slope of this curve is less than that of the 0.5 kip case. This is because the larger value of lateral load induces the second – order geometric effects more quickly. The notional lateral load essentially provides an initial lateral displacement, causing the nonlinear effect to be present at the beginning of the application of the vertical load. These concepts are directly related to the decreased point at which the stiffness of the portal frame assembly begins to decrease rapidly. This point now occurs at approximately 65% to 70% of the elastic critical buckling load. It is at this point that it may be inferred that the portal frame's response is now unstable, with a vertical load of about 10% to

15% less than the 0.5 kip case. It can also be seen that the portal frame does not reach 100% of the elastic critical buckling load. The maximum value of axial load achieved by the system is only approximately 92% of the critical load. Again, this is attributed to the quicker onset of the nonlinear geometric effects as a result of the notional load imposing an initial displacement. Lastly, the curve identifying the notional value multiplied by a value of 3 is considered. Once again it may be seen that a larger initial displacement is imparted to the portal frame. This relates to the second – order geometric effects appearing even quicker and being amplified by the increasing vertical load. As a result, the stiffness curve is unstable in nature throughout its entire trend. The system rapidly loses stability as the vertical load is increased and it achieves a maximum value of only 75% of the elastic critical buckling load. It can be concluded that the initial displacement (i.e. the initial and constant lateral load) has a significant impact on the stiffness and stability of the fixed base portal frame.

The details concerning Figure 2.3.2 (B) are discussed next. First, a major difference in the 0.5 kip, 10% damage case is seen from the Figure 2.3.2 (A) result. It should be noted that the portal frame now buckles in the opposite direction. This is because the effect of the damage to column 1 overtakes the effect of the 0.5 kip lateral load. The portal frame now buckles in its weaker direction, which is toward the left column. It may also be noted that the maximum vertical load achieved by the structure is now only 94% of the elastic critical buckling load. The loss of capacity is directly related to the 10% damage imposed on column 1. The stiffness begins to rapidly decrease around 72% of the elastic critical buckling load, indicating a lower instability point than the virgin condition. The remaining two curves, the notional and 3 times the notional lateral load cases, do not exhibit extreme changes in the response. The notional load case begins to rapidly lose stiffness at approximately the same value of vertical load, 65% to 70% of the

elastic critical buckling load. Again, the structure's response may be considered unstable at this point. The only significant difference for the notional case shown in Figures 2.3.2 (A) and 2.3.2(B) is a loss of capacity of the vertical load of roughly 3%. Similarly, the only significant difference in the 3 times notional load case is approximately a 5% decrease in the maximum vertical load applied. However, it should still be noted that this curve is highly nonlinear and represents a response that is unstable in nature throughout the load application. For these two curves, the response is dominated by the lateral load (i.e. initial displacement), as opposed to the damage imposed on column 1.

The trends described in detail in the previous paragraph are replicated in Figures 2.3.2 (C) and (D). The 0.5 kip case continues to be controlled by the damage imparted to column 1. The 20% and 30% damage scenarios cause rapid loss of stiffness to occur at a lower level of vertical load, and in turn the instability point is decreased. The lowest instability point for the 0.5 kip case is illustrated by Figure 2.3.2 (D) and is approximately at 50% to 55% of the elastic critical buckling load. It should be noted that this curve also only achieves a maximum value of about 86% of the elastic critical buckling load. The remaining two curves again only display slight decreases in the vertical load capacity. The instability point and nonlinear nature of the notional and 3 times the notional load cases remain relatively unchanged by the damage level of column 1. It may be noted that this nature of the response is a trait largely controlled by the direction of the lateral load. If the lateral load had been applied in the direction of the weakened column, the response would be a combination of the damage and second – order geometric effects, as opposed to being dominated by primarily one of the two perturbations.

To conclude the analyses concerned with Load Case #1, it is necessary to ensure that stability failure is the controlling failure mode, versus strength failure. In order for strength

failure to occur, a plastic hinge must be developed at both fixed base supports of the portal frame. A plastic hinge will form when the steel column members are subjected to a reaction moment exceeding the plastic moment, or "M_p." The plastic moment is determined by multiplying the yield stress, "σ_y," by the plastic section modulus, "Z". The plastic section modulus is calculated for the damaged moment of inertia, "$I\alpha$," for each respective damage scenario. It should be noted that this calculation is necessary as a result of the chosen cross – section dimensions utilized in ABAQUS/CAE. To determine if a plastic hinge has developed, the fixed base reaction moments are determined and compared to the plastic moment. The calculations associated with this analysis may be found in Appendix C. If the plastic moment is exceeded, the normalized vertical load level at which it is exceeded is recorded. Table 2.3.1 displays the results obtained by the plasticity analysis.

Table 2.3.1 Normalized Vertical Load Inducing Plastic Hinge Formation Load Case #1

Normalized Vertical Load at Mp (%)			
	0.5 kip	**Notional**	**3X Notional**
0% Damage	-	96	83
10% Damage	97	92	79
20% Damage	93	89	76
30% Damage	88	85	72

The results of the plasticity analysis do indicate that a plastic hinge forms in nearly each case. However, this result is counter intuitive. While at first glance it may seem that strength failure dominates, this is not true given the imposed conditions of the analysis. As previously stated, the lateral displacement of the portal frame is allowed to be a maximum of 1% of the column height. At this displacement, it is easily seen with the aid of Figure 2.3.2 (A-D) that the vertical load does not reach the values displayed in Table 2.3.1. For this reason, it may be

determined that stability is the governing failure mode for the fixed base portal frame. Table 2.3.2 is provided as a further illustration that plasticity is not found within the limits of the study previously described.

Table 2.3.2 Normalized Vertical Load Inducing Lateral Displacement of 1% of Column Height Load Case #1

Vertical Load at Displacement of 1% of Column Height (%)			
	0.5 kip	Notional	3X Notional
0% Damage	-	92	74
10% Damage	94	89	72
20% Damage	92	87	68
30% Damage	87	84	65

It can be seen that all values displayed in Table 2.3.1 are less than those provided in Table 2.3.2. Again, this indicates that the formation of plastic hinges in the portal frame has not occurred. While some cases seem as though the plastic hinge was relatively close to forming, it is important to realize that the vertical load in each case exceeds 50% of the elastic critical buckling load. In practice, this is not common. Several factors of safety limit this value well below the critical load. Also, vertical loads are typically constant in most building structures, whereas this study linearly increases the load. The details provided in Load Case #2 suggest a much more likely load scenario encountered by building structures.

The second load case applied to the fixed base portal frame is defined by an initial and constant vertical load, followed by a linearly increasing lateral load. Again, the loads are treated as point forces, the vertical load being applied to the top joints of both column 1 and 2, whereas the lateral load is applied only to column 1. This load case will hereafter be referred to as Load Case #2.

The lateral load begins at a value of 0 and is linearly increased to a maximum value of 100 kips. Several different values are assigned to the constant initial vertical load in Load Case

#2. In practice, columns are rarely subjected to axial loads exceeding 50% of their respective elastic critical buckling load. For this reason, values of the vertical load were chosen to be 10%, 30%, and 50% of the virgin state elastic critical buckling load of the fixed base portal frame. The lower value of 10% represents a case where the second – order geometric effects of the frame are minimized, while the upper value of 50% represents a case where these effects pose a major contribution to the response of the system. Load Case #2 is a more realistic loading scenario similar to an actual structure supporting a constant gravity load and subjected to a lateral load event. It is expected that the larger magnitude of the lateral load utilized in Load Case #2 will illustrate a response largely controlled by the second – order geometric effects.

Hazard – independent damage scenarios of 0%, 10%, 20%, and 30% are analyzed once again. The damage levels are with respect to the bending resistance of column 1 only. The procedure for determining the reduced moment of inertia for use in ABAQUS/CAE is identical to that discussed in the previous paragraphs related to Load Case #1.

Figure 2.3.3 is provided as a summary of the concepts related to Load Case #2. The variable "P_0" indicates the initial, and constant, vertical load. The linearly increasing value of the lateral load is indicated by the variable "F." Lastly, the red circle surrounding column 1 illustrates the member receiving the hazard – independent damage. Once again, for the geometry and section assignments of the fixed base portal frame, please refer to Figure 2.2.1.

Figure 2.3.3 Load Case #2 & Hazard - Independent Damage Application

Figure 2.3.4 provides the results of the stiffness/stability analysis of the fixed base portal frame subjected to Load Case #2. Similar to Figure 2.3.2, the lateral displacement of the frame assembly is normalized by the column height, and the lateral load is normalized by the virgin state elastic critical buckling load. The upper boundary of the lateral load is once again limited to 1% of the column height. It should be noted that the lateral load is now the primary variable of the stiffness plots, as opposed to the vertical load as seen in Figure 2.3.2. Deformed shapes, at a value scale factor of 1, are also provided along with the stiffness curves. Lastly, the identifiers A, B, C, and D define the damage scenarios of 0%, 10%, 20% and 30%, respectively.

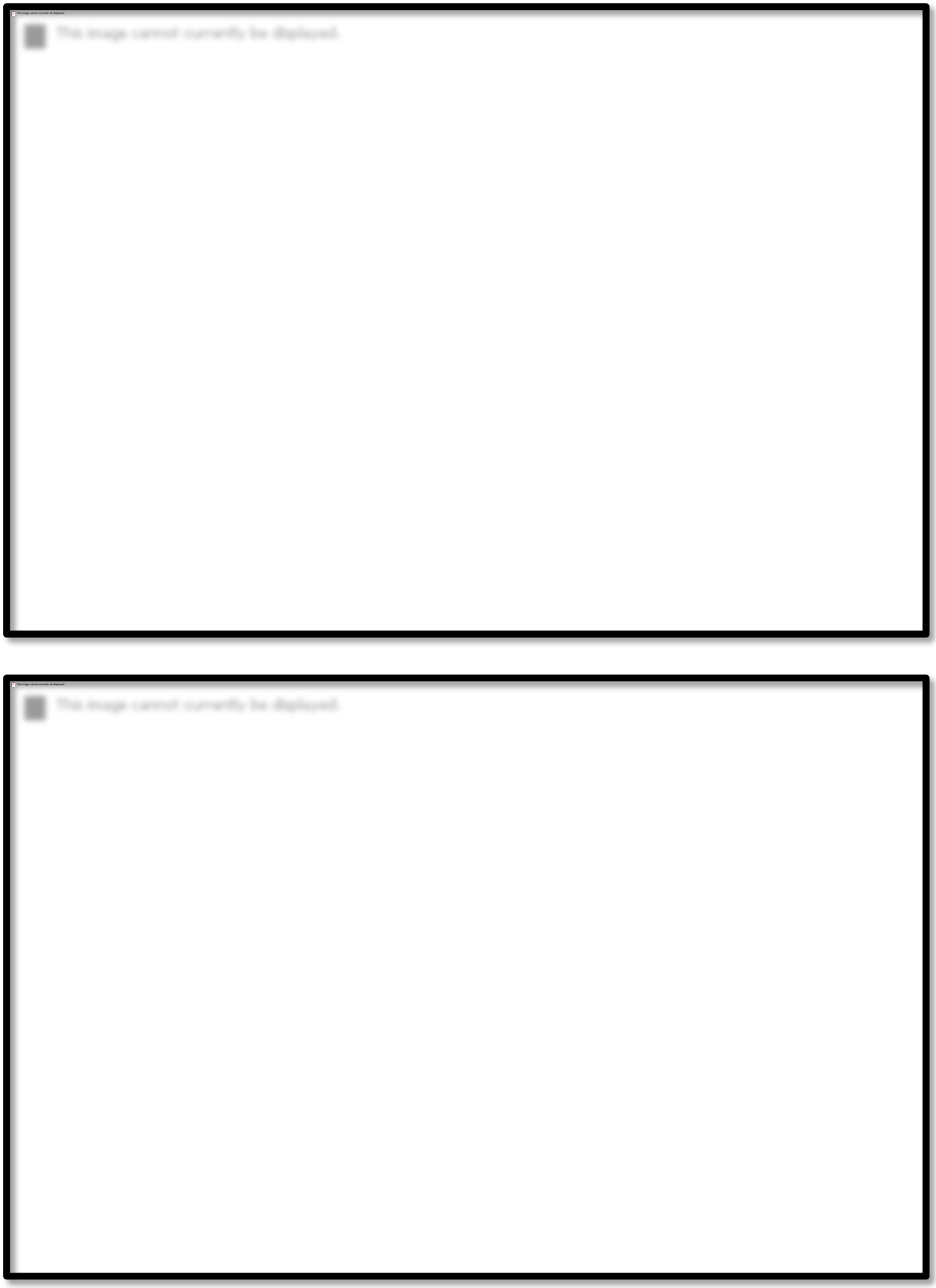

Figure 2.3.4 Stiffness Curves Due to Load Case #1: (A) Virgin State (B) 10% Damage (C) 20% Damage (D) 30% Damage

Figure 2.3.4 Stiffness Curves Due to Load Case #1: (A) Virgin State (B) 10% Damage (C) 20% Damage (D) 30% Damage

Several conclusions may be drawn from the results of Figure 2.3.4. First, it may be noted that the maximum value of the lateral load for each load case decreases as the hazard – independent damage of column 1 increases. That is, the maximum value of the lateral load for each load case is shown by Figure 2.3.4 (A), the 0% damage case, whereas the minimum lateral load for each case is shown by Figure 2.3.4 (D). It may also be noted that a different slope appears as a result of the value of the vertical load. Simply, the slope, or stiffness, of the response curves depends on the value of the vertical load. The slope value decreases as the value of the vertical load increases. This is directly a result of the amplification of the nonlinear geometric effects induced through an increase in the column axial loads. For this reason, the maximum system stiffness is shown by the 10% elastic critical buckling load case. Inversely, the minimum system stiffness is shown by the 50% elastic critical buckling load case. Although the responses shown in Figure 2.3.4 may appear linear in nature, it is the second – order geometric effects that result in the different slopes, or stiffnesses, of the load cases. Lastly, it may be noted that the stiffnesses of each load case do not change significantly with an increase in the hazard – independent damage. This is because the second – order geometric effects dominate the system's response. The magnitude of lateral load causes a nonlinear geometric effect that overtakes the imparted damage effect. If the lateral load were applied in the direction of the weakened column, the solution would once again become a combination of these effects, as opposed to only one of the perturbations.

A plastic hinge check is once again performed in order to ensure that stability failure governs the fixed base portal frame as opposed to strength failure. The reaction moments at the fixed bases are obtained and it is verified that the plastic moment is not exceeded. The calculations involved with this analysis are provided in Appendix C. Table 2.3.3 provides the

normalized lateral load at which plastic hinge formation occurs. As expected, stability failure governs within the lateral displacement of 1% of column height boundary. The values of lateral load shown in Table 2.3.3 induce a lateral displacement that is beyond the bounds of this analysis.

Table 2.3.3 Normalized Vertical Load Inducing Plastic Hinge Formation Load Case #2

Lateral Load at Mp (%)			
	0.1 Pcr	0.3 Pcr	0.5 Pcr
0% Damage	2.58	2.10	1.56
10% Damage	2.41	1.93	1.42
20% Damage	2.27	1.78	1.30
30% Damage	2.10	1.67	1.16

Table 2.3.4 provides the lateral load values at which a lateral displacement of 1% of the column height occurs. The results of this table are significantly lower than those found in Table 2.3.3. This further verifies that plastic hinge formation does not occur in the fixed base portal frame. In the conditions defined for the analyses performed in this section, stability governs the failure of the frame system.

Table 2.3.4 Normalized Vertical Load Inducing Lateral Displacement of 1% of Column Height Load Case #1

Lateral Load at Displacement of 1% of Column Height (%)			
	0.1 Pcr	0.3 Pcr	0.5 Pcr
0% Damage	2.01	1.56	1.13
10% Damage	1.93	1.50	1.08
20% Damage	1.84	1.42	0.99
30% Damage	1.76	1.33	0.91

The studies involving the fixed base portal frame are concluded in this section. A 4 story – 2 bay planar frame model is subjected to additional stability studies in the following chapter.

3. COMPUTATIONAL FEA OF 4 STORY – 2 BAY STEEL FRAME

3.1 Elastic Critical Buckling Load Analysis and Model Formulation

Chapter 3 of this work begins by extending the stability and stiffness analyses performed in the previous chapter to a more complex steel planar frame model. Specifically, the frame model contains 4 stories and 2 bays. An elastic critical buckling load analysis is performed to investigate members of the frame system that are likely sensitive to damage and could create potential stability issues. Hazard – independent damage scenarios are derived from the result of the buckling analysis. Finally, the steel frame section properties and the applied loadings are detailed. All modeling procedures are completed utilizing ABAQUS/CAE.

In an effort to generalize the study as much as possible, a typical steel frame designed for high velocity wind areas is utilized. This design has been verified through an outside party, and the actual design of the steel members is not performed within this work. Figure 3.1.1 is provided along with Table 3.1.1 to detail the geometric orientation of the frame and the corresponding steel section assignments.

Table 3.1.1 Steel Section Designations

Steel W-Shape Frame Members	
A	W12x79
B	W21x62
C	W10x68
D	W18x40
***Columns are 144" in Height**	
****Beams are 150" in Length**	

Figure 3.1.1 4 Story - 2 Bay Steel Frame with Section Designations & Applied Loadings

The designation "A-D" may be seen for each section in the table, and its corresponding location may be found within the figure. It should be noted that the beams and columns of the 1st floor of the frame are slightly stiffer than the sections found in the stories above. This selection is a result of these members being subjected to the cumulative loads from the floors above. For simplicity, the frame is again chosen to be supported through fixed bases at the ground level. As stated in Table 3.1.1, each beam is 150" in length, and each column is 144" in height. While the applied loading of the frame model appears in Figure 3.1.1, it is not of interest yet, and will be further discussed in the following paragraphs.

After defining the steel frame model, the elastic critical buckling load analysis may begin. This procedure is completed using the predefined eigenvalue/buckling step in ABAQUS/CAE. The principle of bifurcation of equilibrium as detailed in previous discussions is the theory utilized in this analysis. The elastic critical buckling load obtained from this investigation is that which causes the global stiffness matrix to be of null value. At this critical

load, the second – order geometric effects have overtaken the system response, and the lateral displacement of the system begins to increase without bound. Figure 3.1.2 provides the application of the loads for the elastic critical buckling load analysis associated with the steel frame.

Figure 3.1.2 Elastic Critical Buckling Load Analysis & Associated Unit Loads

It should be noted that unit loads, or fractions of unit loads, are the only loads present in this analysis. The interior columns of the 1st through 3rd floors receive a value of 1 kip, as opposed to the exterior columns, which receive 0.5 kips. This is because the center column has twice the tributary length than the exterior columns. Also, the 4th floor is given half of the values corresponding to the floors below it. This is a result of the 4th floor being treated as the roof of the structure. This assumption provides reasoning to apply only a fraction of the loading that the actual inhabitable floors receive. By utilizing the loads displayed in Figure 3.1.2 for the buckling analysis, it is possible to obtain maximum value of the frame system buckling load. That is, the loads with a value of 1 will receive the actual eigenvalue/critical load, whereas the other point loads will receive a fraction of this load. This method of analysis provides a less cumbersome

and more intuitive result for the elastic critical system buckling load. The computational model is developed using the details provided in this section, and the elastic critical buckling load is executed. Figure 3.1.3 provides the obtained buckling loads and their respective deformed shapes for the first 3 buckling modes of the steel frame.

Figure 3.1.3 Critical Buckling Loads & Deformed Configurations: Modes 1-3

As expected, a significant increase in the elastic critical buckling load arises between the three mode shapes. Buckling Mode 1 will occur first, at a load of approximately 1753 kips. At nearly a 1000 kip increase in the applied load, Buckling Mode 2 occurs at 2820 kips. Lastly, the highest load, Buckling Mode 3 occurs at a value of 3460 kips. Careful consideration should be taken to note that the obtained buckling loads are with respect to the unit loads found in Figure 3.1.2. It is evident through this analysis that Buckling Mode 1 is the most critical case for the planar steel frame. A significantly large increase in the gravity loads imposed on the frame

system is necessary for a higher buckling mode to occur. Because this is not a likely condition to occur in building structures, both the higher Buckling Modes 1 and 2 are disregarded for further investigation. Buckling Mode 1 is chosen as the motivation for the hypothetical damage scenarios.

Upon examining the deformed configuration of Buckling Mode 1, a pivotal conclusion may be drawn. The actual buckling phenomenon appears to occur to the 2nd floor columns. That is, the second – order geometric effects are amplified by the applied loading, and the lateral displacement of these columns begins to increase without bound. Therefore, it may be postulated that the stability of the planar steel frame may be sensitive to a damage event at the 2nd floor level. Weakening of these columns will result in buckling at a lower magnitude of vertical load. Through the studies performed in Chapter 2, it may be seen that the presence of a lateral load will only worsen these effects on the stability and stiffness of the system.

Three hazard – independent damage scenarios affecting the 2nd floor columns are chosen for the stability analyses performed in this chapter. The first hazard – independent damage scenario investigated applies damage to only the left exterior 2nd floor column of the steel frame. As an example, this damage could be created through a wind event in the form of a concentrated pressure, or a wind – driven projectile. The second hazard – independent damage scenario applies damage to the interior column of the 2nd floor. Once again, a possible event that could produce this damage is an interior blast. The last hazard – independent damage scenario applies damage to all columns of the 2nd floor. This type of damage could be caused through seismic excitation of a fundamental mode activating the 2nd floor drift. While examples that could cause the proposed damage scenarios are given, the important concept to recall is that the damage is, by definition, hazard – independent. The methods detailed could be utilized for any number of

damage scenarios. The three cases chosen were based simply on Buckling Mode 1. Figure 3.1.4 depicts the three damage scenarios to be examined in this chapter. The orange circle indicates the exterior column damage scenario. The green circle indicates the interior column damage scenario. Lastly, the red circle indicates scenario damaging all 2nd floor columns.

Figure 3.1.4 Hazard-Independent Damage Scenarios

Before beginning the stability analysis of the hazard – independent damage scenarios, it is necessary to define a load case to apply to the planar steel frame. Attention is first turned to the formulation of the gravity loads. As stated previously, the frame being analyzed is a typical design for high velocity wind areas. Therefore, abnormal values of gravity loads are not the focus of this study. Rather, loads that are applied to building structures throughout their lifetime are within the scope of this research. This leads to the development of the common gravity load designations, dead and live loads. It is assumed that the 1st floor contains a typical concrete slab, while the upper floors are optimized using composite slabs. These slabs account for the majority of the dead load imposed on the frame, and are therefore the only dead load calculated for load

development in this study. The unit weights, thicknesses, and respective lengths of the floor slabs are displayed in Table 3.1.2.

Table 3.1.2 Dead Load Variables & Calculations

Dead Load							
		Unit Weight	Thickness	Out-of-Plane Length	In-Plane Length	Contingency	Point Load
		PCF	In.	Ft.	Ft.	%	Kips
1st Floor		150	10	20	12.5	5	32.8125
	Steel	-	-	-	-		
2nd Floor	Concrete	150	4	20	12.5	5	23.84375
	Steel	490	1	20	12.5		
3rd Floor	Concrete	150	4	20	12.5	5	23.84375
	Steel	490	1	20	12.5		
4th Floor	Concrete	150	4	20	12.5	5	23.84375
	Steel	490	1	20	12.5		

Upon viewing the table above, it should be noted that a contingency of 5% is included in the dead load calculation to account for the frame's façade and any uncertainties. The results of dead load development are point forces that will be applied vertically to the joints of the frame system.

Next, the live load to be applied to the planar steel frame is derived. It is necessary to consult the ASCE manual entitled, "Minimum Design Loads for Buildings and Other Structures" for accurate consideration of this load. For simplicity, all floors of the structure are chosen to be an "office" type live load with the exception of the 4^{th} floor. Again, this floor is considered as the roof of the structure and for this reason, it is given a "roof" type live load. The values and associated calculations developing the live load applied to the planar steel frame are shown in Table 3.1.3.

Table 3.1.3 Live Load Variables & Calculations

Live Load					
	Type	Unit	Out-of-Plane Length	In-Plane Length	Point Load
	-	PSF	Ft.	Ft.	Kips
1st Floor	Office	50	20	12.5	12.5
2nd Floor	Office	50	20	12.5	12.5
3rd Floor	Office	50	20	12.5	12.5
4th Floor	Roof	20	20	12.5	5

As a final step in developing the gravity load case, the dead and live loads are summed in order to obtain total gravity load point forces. The results of this step, along with an abbreviation corresponding to the point loads, are displayed in Table 3.1.4. The abbreviations of the point forces may be utilized in reference to Figure 3.1.1 to illustrate their locations on the frame system. As a final note concerning the gravity load case applied to the structure, it should be known that a load factor is not applied. This is avoided so as to provide an applied loading that is similar to what the typical building structure is frequently subjected to.

Table 3.1.4 Total Gravity Loads & Corresponding Abbreviations

Total Gravity Load				
	Dead Load	Live Load	Total Point	
	Kips	Kips	Kips	Abbreviation
1st Floor	32.8125	12.5	45.3125	DL + LL (1)
2nd Floor	23.84375	12.5	36.34375	DL + LL (2)
3rd Floor	23.84375	12.5	36.34375	DL + LL (2)
4th Floor	23.84375	5	28.84375	DL + LL (3)

To complete the derivation of the load case to be applied to the planar steel frame, a lateral load is developed. Once again, the ASCE manual "Minimum Design Loads for Buildings and Other Structures," is necessary for accurate application of this load. Because the frame system being analyzed is typical for a high velocity wind area, the lateral load chosen for development is that of wind. Table 3.1.5 provides the assumptions and calculations necessary to

develop a gust pressure for application as a lateral load. It should be noted that the values of the variables shown in this table were chosen to provide the most generalized gust applicable to the low – rise steel planar frame.

Table 3.1.5 Wind Gust Variables and Calculations

Gust - Wind Calculation						
	Factor	K_z	K_{zt}	K_d	V^2	Q
	-	-	-	-	MPH	PSF
All Floors	0.00256	0.8	1	0.85	170	50.31

As a final step in developing the lateral load, the obtained gust pressure is converted to a series of point loads for application to the frame system. The resulting point loads, along with their respective tributary lengths are provided in Table 3.1.6. The abbreviation for the respective point loads are provided once more as a reference for their location on the frame system using Figure 3.1.1. Again, it should be noted that the resulting lateral loads are not amplified by a load factor. This is again avoided to provide a lateral load that is within the design limits of the structural system.

Table 3.1.6 Lateral Load Variables & Calculations with Corresponding Abbrevations

Lateral Load					
	Q	Out-of-Plane Length	In-Plane Height	Point Load*	
	PSF	Ft.	Ft.	Kips	Abbreviation
1st Floor	50.31	20	14	14.4	F(1)
2nd Floor	50.31	20	14	14.4	F(1)
3rd Floor	50.31	20	14	14.4	F(1)
4th Floor	50.31	20	7	7.2	F(2)
***Load is result of rounding to nearest kip per linear inch in calculation**					

The application of the gravity load and lateral load to the steel planar frame follows identically to Load Case #2 in Chapter 2 of this work. As an initial step, the total gravity load is linearly increased from a value of 0 to its maximum value provided in Table 3.1.4. Next, the

lateral load is increased linearly from a value of 0 to its maximum value provided in Table 3.1.6. This series of loading was chosen to provide a scenario that is similar to what an actual building structure commonly experiences. The option allowing the analysis to include second – order geometric effects during the load application is chosen in ABAQUS/CAE. Also, the hazard – independent damage is applied in this program through a reduction in the modulus of elasticity of the steel frame members. In simple terms, a hazard – independent damage scenario resulting in 20% damage is applied through a 20% reduction in the modulus of elasticity in the frame member receiving the damage. This can be seen as an effective "αE," versus the effective "αI" imposed in Chapter 2. By affecting the modulus of elasticity, the stiffness associated with each degree of freedom of the frame member is reduced.

A final step is completed before beginning the stability analysis of the 4 story – 2 bay frame. To ensure that the planar frame is within design limitations, the interaction equation provided by the American Institute of Steel Construction is checked. This calculation ensures that the combined effects of the axial load and bending moment applied to any of the columns falls below its respective design capacity. The "worst case" column, the 1st floor interior column, is chosen for this calculation. First the maximum applied axial load and bending moment to this column is found using ABAQUS/CAE. Next, the design capacity of both the bending moment and axial load of the steel section associated with this column is obtained from the Steel Construction Manual. The ratio of the applied load and bending moment to the axial load and bending moment capacity of the column is calculated. The obtained result is checked to ensure that the ratio is less than or equal to 1. Table 3.1.7 provides the result of this analysis.

Table 3.1.7 Interaction Design Check of 1st Floor Interior Column

Design Capacity Check				
Pr	Pc	Mr	Mc	Interaction
Kip	Kip	Kip Ft.	Kip Ft.	-
290	887	142	438	0.62

It may be noted that the interaction result is 0.62, leaving a reserve capacity of roughly 40%. This result ensures that the loads developed in the previous section do not pose a direct threat to the strength design of the frame. Because a large reserve capacity is seen in this frame member, the plasticity checks performed in Chapter 2 are not performed for this study. Also, a form of plasticity is implied through the application of the hazard – independent damage on the modulus of elasticity of the frame members. For this reason, plasticity checks are not valid, but an effort is instead made to illustrate that an effective design of the planar has been met. The following sections provide the results of the stability analyses performed for each hazard – independent damage scenario.

3.2 Stability Sensitivity: Hazard-Independent Damage of 2nd Floor Exterior Column

In this section of Chapter 3, the hazard – independent damage application to the 2nd floor exterior column and its effects on the stability of the planar steel frame are investigated. For the development of the steel frame model, applied loads, and damage scenarios, please refer to Section 3.1.

Several damage levels to the 2nd floor exterior column are investigated to gain a broader understanding of the system's sensitivity to the damage scenario. The values are 0%, 20%, 40%, 60%, and 80% damage. Again it should be noted that the damage is now applied through a reduction in the modulus of elasticity, and therefore it effectively reduces the stiffness of all degrees of freedom associated with a particular frame element. Identical load cases are analyzed for each damage level. That is, the only variable changing in the analyses performed is the level of the hazard – independent damage.

Upon creating the computational model in ABAQUS/CAE, the loads are applied and the lateral displacement of the 2nd floor and 4th floor are tracked. The lateral displacement of the 2nd floor is tracked so as to obtain the effect of the damage to the 2nd floor exterior column on the inter-story drift. That is, the relative displacement between the 1st floor and 2nd floor is investigated. The lateral displacement of the 4th floor is tracked so as to provide a means of examining how the damage affects the total drift of the 4 story frame. The values of the 2nd floor inter-story drift and the 4th floor total drift are normalized by percent of column height and percent of total frame height, respectively. The lateral load corresponding to the 2nd floor and 4th floor are also tracked throughout the analyses. Their values are normalized by the total cumulative shear force acting at the corresponding floor. That is, the 4th floor value is normalized by the total lateral load on the frame system, while the 2nd floor value is normalized

by the sum of the lateral loads on the 4th, 3rd, and 2nd floors. The results of the lateral displacements of the 2nd and 4th floors after the application of damage to the 2nd floor exterior column are provided in Figure 3.2.1. The deformed configurations are also provided at a scale factor of 20.

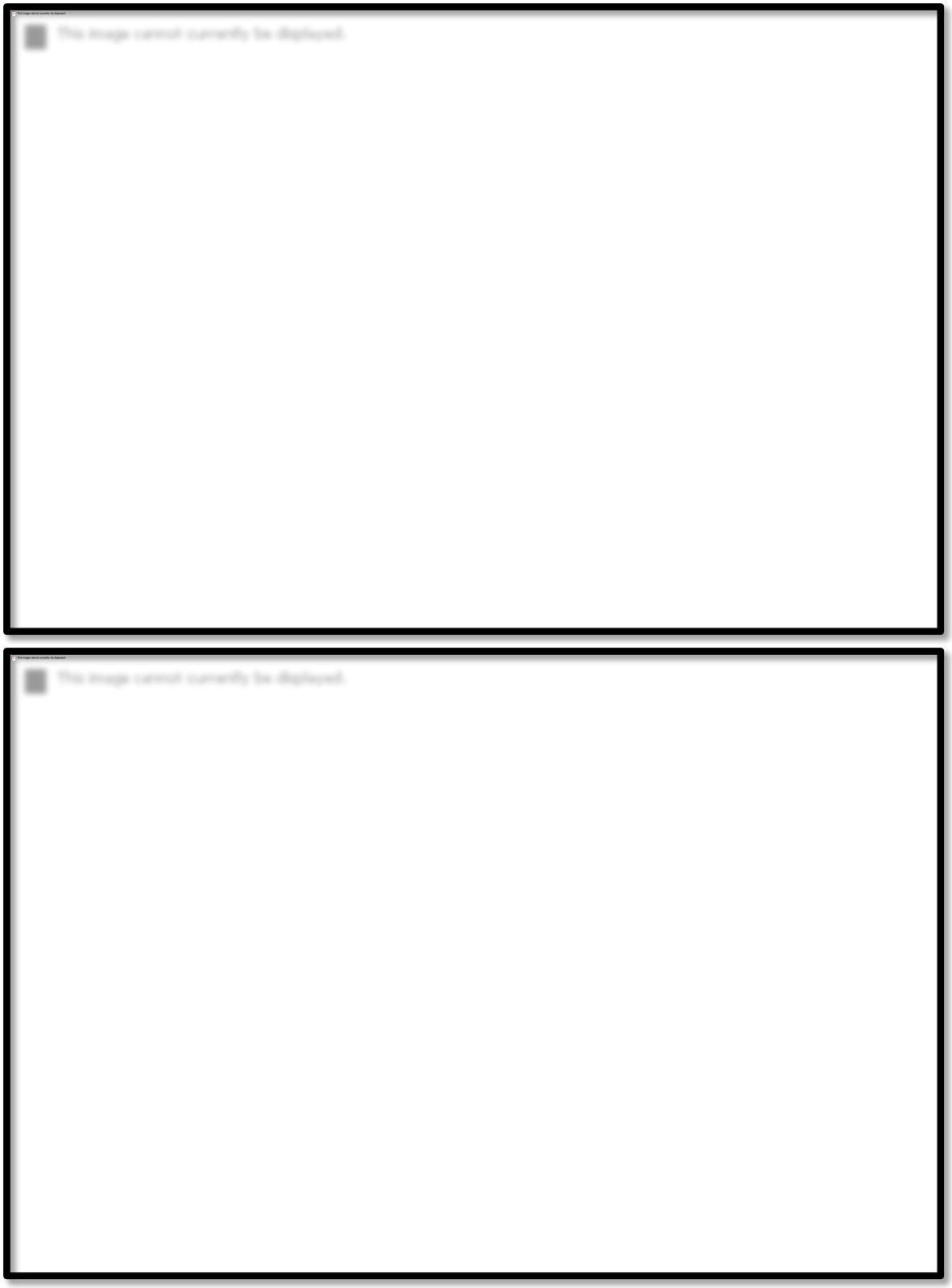

Figure 3.2.1 (A) Inter-Story Drift of 2nd Floor (B) Total Drift of 4th Floor

Attention is first directed to the inter-story drift of the 2nd floor, as shown in Figure 3.2.1 (A). While an effect is seen on the inter-story drift, it is not profound. The maximum damage case of 80% results in an inter-story drift of only 0.6% of the column height. This value is only about a 20% increase from the virgin condition. The results would suggest that the planar steel frame is not highly sensitive to the damage of the exterior 2nd floor column. However, this result is largely dependent on the directionality of the applied loading. If the lateral load were applied from right to left, the impact of this damage scenario would likely be much greater. Therefore, the obtained result is valid only under the loading conditions described in this chapter. It should also be noted that the 100% damage level was not investigated because of its misleading result. Due to this same directionality effect, the inter-story drift would appear to decrease at this level. This is because a large initial inter-story drift in the negative direction would occur, and the applied lateral load would result in a final inter-story drift value that is in the positive direction, but of low magnitude. The low magnitude would be a result of "pushing" the structure back in the direction of its unreformed configuration.

Next, the total drift of the 4 story – 2 bay frame system shown in Figure 3.2.1 (B) is examined. The results show almost no discernible effect on the total drift of the frame system. With reference to the direction of the applied loading, the combined results of Figure 3.2.1 would suggest that sensitivity to damage of the 2nd floor exterior column does not exist.

As an additional post-processing analysis, the changes in the slope, or stiffness, of the inter-story drift and total drift responses as a result of the damage is of interest. Figure 3.2.2 illustrates the loss of stiffness versus the percent damage applied to the exterior column of the 2nd floor for both the inter-story and total drift cases.

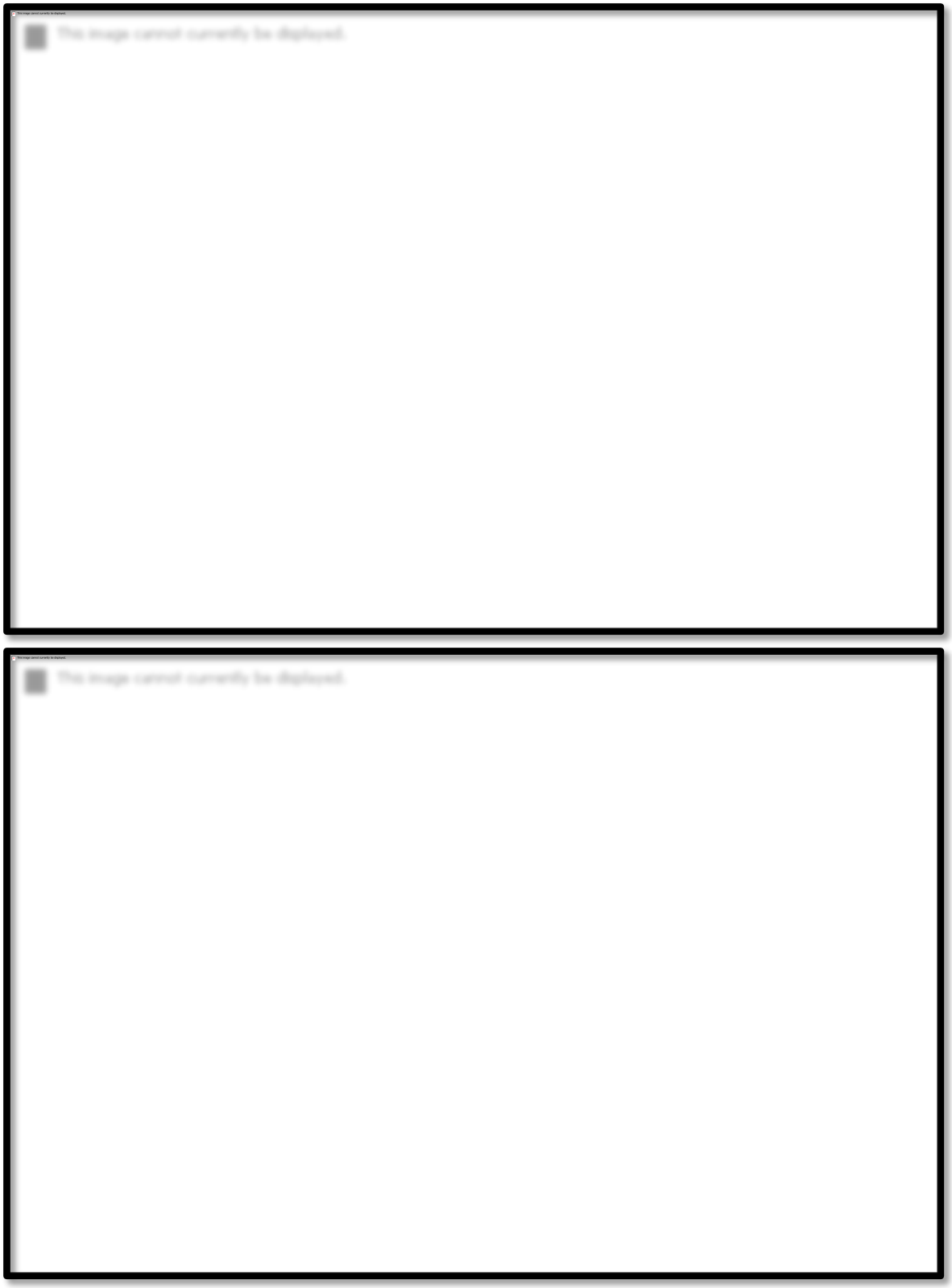

Figure 3.2.2 Loss of Stiffness vs. Percent Damage (A) 2nd Floor (B) Global

Upon investigating Figure 3.2.2, several conclusions may be drawn. First, the highest damage value, 80%, results in about a 15% loss of stiffness concerning the inter-story drift of the 2nd floor. While this is not a desirable loss, it is certainly not devastating. A similar result is found concerning the total drift of the system. An 80% damage value to the exterior 2nd floor column results in approximately 3% loss of the global stiffness of the system. Again, this loss is far from critical and the planar frame assembly is still quite stable under this particular damage scenario. Once again, it should be noted that this result is unique to the applied loading direction and is subject to change if the loading scenario is modified. The damage scenario affecting the interior column of the 2nd floor is investigated in the following section.

3.3 Stability Sensitivity: Hazard-Independent Damage of 2nd Floor Interior Column

In this section of Chapter 3, the hazard – independent damage application to the 2nd floor interior column and its effects on the stability of the planar steel frame are investigated. For the development of the steel frame model, applied loads, and damage scenarios, please refer to Section 3.1.

Similar to the previous section, several damage levels are imparted to the interior column of the 2nd floor to obtain a complete investigation of the effects of this particular damage scenario. The values are 0%, 20%, 40%, 60%, 80%, and 100% damage. Damage is again applied through the reduction of the modulus of elasticity of the member receiving damage. The load case applied to the frame system continues to remain unchanged from that defined in Section 3.1.

The inter-story drift of the 2nd floor and the total drift of the 4th floor remain the primary variables investigated throughout the analyses. The development of the lateral load applied to these floors also remains an important variable in the study. Both the story drifts and lateral loads are normalized using the same techniques defined in Section 3.2. The results of the lateral displacements of the 2nd and 4th floors after the application of damage to the 2nd floor interior column are provided in Figure 3.3.1. The deformed configurations are also provided at a scale factor of 20.

Figure 3.3.1 (A) Inter-Story Drift of 2nd Floor (B) Total Drift of 4th Floor

The results of the damage effect on the inter-story drift, as shown in Figure 3.3.1 (A), are investigated first. A more profound effect on the 2nd floor inter-story drift is seen as a result of damaging the 2nd floor interior column as opposed to the exterior column. The maximum damage value, 100%, yields a drift value of approximately 0.85% of the column height. This is nearly a 90% increase in the inter-story drift value obtained in the virgin condition. This is certainly a result largely dependent on the "sagging" effect created on the 2nd floor. As the interior column is weakened, its axial capacity is reduced. This allows the 2nd floor beams to displace downward, pulling the frame structure toward its centerline. This effect "pulls" the structure in the same direction that the lateral load is attempting to displace it. Therefore, the inter-story drift is amplified as a result of the two actions acting simultaneously. This result is not impacted by the direction of the lateral load, due to the symmetry of the imposed damage.

Next, the results of the damage effect on the total drift of the 4th floor, as shown in Figure 3.3.1 (B), are investigated. Once again, the effect of the interior column damage is greater than that seen in the exterior column damage case. The 100% damage value produces a total drift value of approximately 0.40% of the total frame height. This is about a 30% increase of the total drift obtained in the virgin state. While its effect on the total drift is less than that of the inter-story drift, the interior column damage certainly affects the response of the structure. This again may be attributed to the "sagging" effect.

The changes in the slope, or stiffness, of the inter-story drift and total drift responses as a result of the damage is again analyzed. Figure 3.3.2 illustrates the loss of stiffness versus the percent damage applied to the interior column of the 2nd floor for both the inter-story and total drift cases.

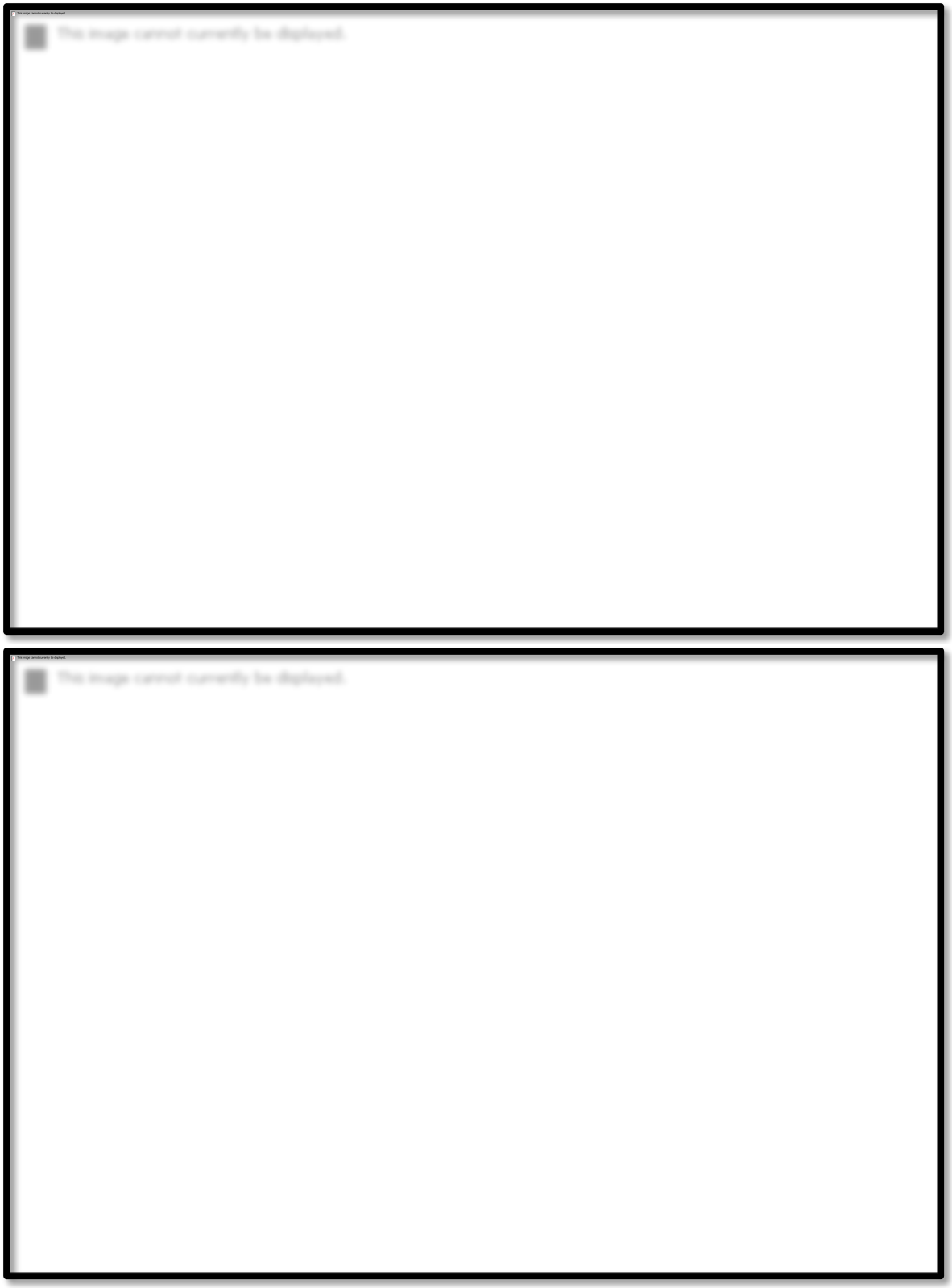

Figure 3.3.2 Loss of Stiffness vs. Percent Damage (A) 2nd Floor (B) Global

After imposing 100% damage to the interior column of the 2nd floor, approximately 40% loss of the 2nd floor stiffness may be seen. Upon viewing Figure 3.3.2 (A), the result suggests that a critical value of approximately 60% damage initializes the rapid onset of instability. That is, the stiffness of the 2nd floor begins to reduce dramatically with small increases in the damage applied to the interior column. Figure 3.3.2 (B) suggests a similar result. Imposing 100% damage to the interior column of the 2nd floor results in approximately 25% loss of the global stiffness of the frame. The critical value of damage causing rapid onset of instability is about 80%. The following section investigates the stability of the frame system after imposing damage to all 2nd floor columns.

3.4 Stability Sensitivity: Hazard-Independent Damage of All 2nd Floor Columns

In the final section of Chapter 3, the hazard – independent damage application to all of the 2nd floor columns and their effect on the stability of the planar steel frame are investigated. For the development of the steel frame model, applied loads, and damage scenarios, please refer to Section 3.1.

The damage values of 0%, 20%, 40%, 60%, and 80% are imposed on the 2nd floor columns. The 100% damage scenario is not investigated, as this would lead to the collapse of the 2nd floor, and therefore stability is no longer a relevant concern. Damage is once again applied through the reduction of the modulus of elasticity of the member receiving damage. The load case applied to the frame system continues to remain unchanged from that defined in Section 3.1.

The inter-story drift of the 2nd floor and the total drift of the 4th floor remain the primary variables investigated throughout the analyses. The development of the lateral load applied to these floors also remains an important variable in the study. Both the story drifts and lateral loads are normalized using the same techniques defined in Section 3.2. The results of the lateral displacements of the 2nd and 4th floors after the application of damage to all of the 2nd floor columns are provided in Figure 3.4.1. The deformed configurations are also provided at a scale factor of 20.

Figure 3.4.1 (A) Inter-Story Drift of 2nd Floor (B) Total Drift of 4th Floor

The results of the damage effect on the inter-story drift, as shown in Figure 3.4.1 (A), are investigated first. As expected, the planar frame is highly sensitive to the all 2nd floor column damage case. The maximum damage value, 80%, yields a drift value of approximately 1% of the column height at a normalized lateral load value of 75%. This result indicates the inter-story drift has reached a critical value prior to the maximum lateral load. Stability then, is a major concern for this damage scenario. When compared to the virgin state inter-story drift, approximately 110% increase is seen by the 80% damage scenario. It should also be noted that a larger difference may be seen between each damage level. That is, the inter-story drift increases exponentially with an increase in the damage level. Unlike the exterior column damage scenario, this result is not dependent on the direction of the lateral load. This is due to the symmetry of the imposed damage.

Next, the results of the damage effect on the total drift of the 4th floor, as shown in Figure 3.4.1 (B), are investigated. Similar to the inter-story drift result, this damage scenario has a rather large effect on the system response. The 80% damage value produces a total drift value of approximately 0.59% of the total frame height. This is about a 100% increase of the total drift obtained in the virgin state. From the results of both the inter-story and total drift values, it may be determined that the all 2nd floor column damage scenario has a devastating impact on the stability of the planar steel frame.

The changes in the slope, or stiffness, of the inter-story drift and total drift responses as a result of the damage is once again analyzed. Figure 3.4.2 illustrates the loss of stiffness versus the percent damage applied to all of the 2nd floor columns for both the inter-story and total drift cases.

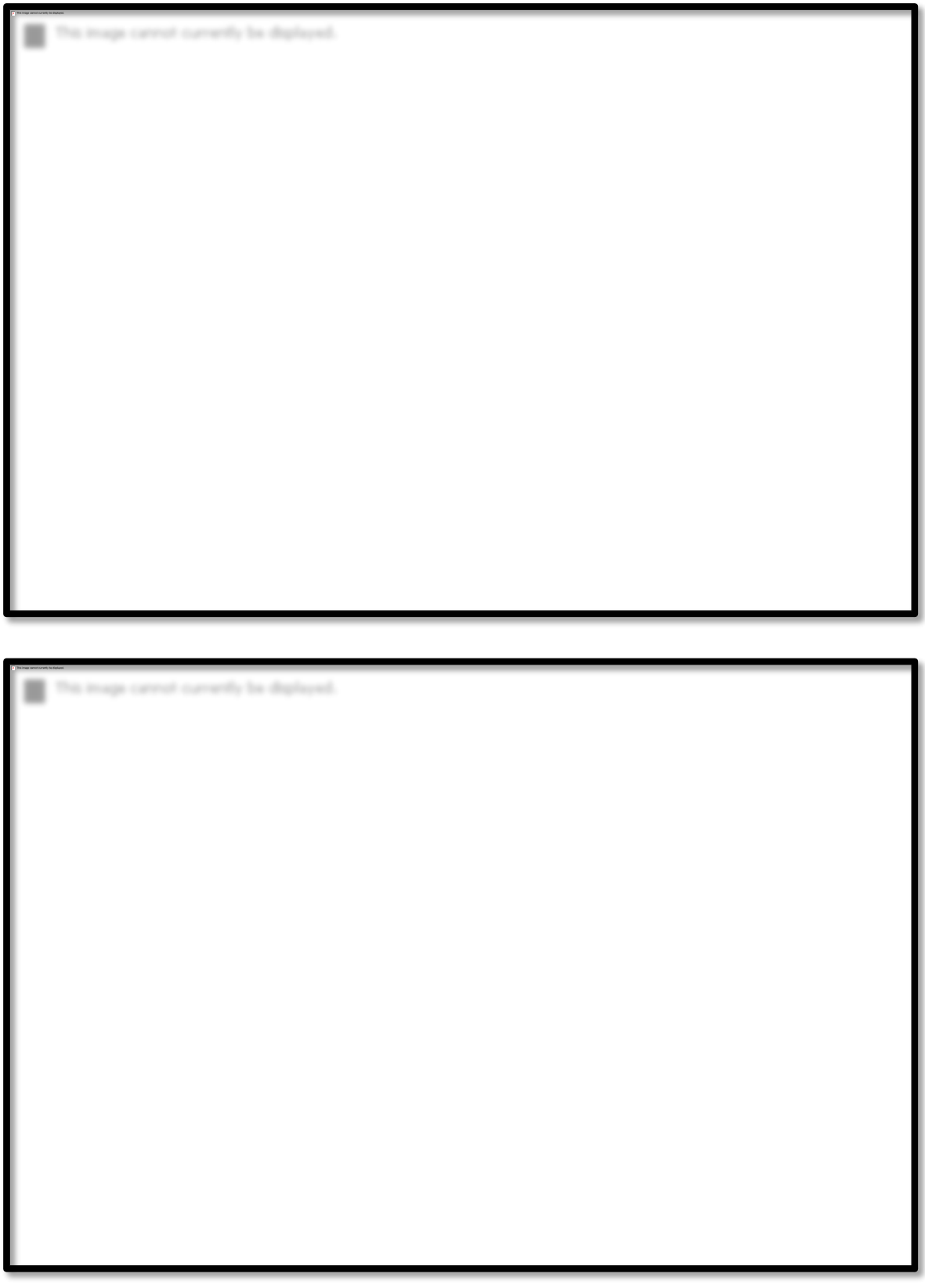

Figure 3.4.2 Loss of Stiffness vs. Percent Damage (A) 2nd Floor (B) Global

Upon examining the results of Figure 3.4.2, several conclusions may be made. Both curves are unstable in nature and illustrate the large effect of this particular damage scenario on the frame's response. Considering the 2nd floor stiffness, a slightly more constant loss of stiffness may be seen. The damage effect is not linear; however a definite trend is obtained. As a rough estimate, any particular damage value leads to a loss of stiffness of about half of the same value. The trend displayed by this case suggests that even a small value of damage could result in loss of stability. Another highly nonlinear trend is obtained in Figure 3.4.2 (B). From this, it may be inferred that the all 2nd floor column damage scenario greatly impacts the loss of global stiffness. Additionally, the rapid onset of instability may be seen at a critical damage level of approximately 70%. The following chapter extends the stability investigations to a three – dimensional steel – moment frame system.

4. COMPUTATIONAL FEA OF LOW-RISE STEEL FRAMED BUILDING

4.1 Model Formulation

Chapter 4 of this work begins by extending the stability and stiffness analyses performed in the previous chapter to a three – dimensional steel – moment framed building. More precisely, 7 of the 4 story – 2 bay planar frames defined in Chapter 3 are connected in parallel with the addition of longitudinal girders. Three – dimensional, hazard – independent damage scenarios are extrapolated from the planar damage scenarios also defined in Chapter 3. ABAQUS/CAE is once again utilized for all modeling procedures performed within this chapter.

The typical steel frame designed for high velocity wind areas defined in Chapter 3 is utilized to create the three – dimensional framing system. Once again, it should be noted that the design has been verified through an outside party, and the actual design of the steel members is not performed within this work. Please refer to Figure 3.1.1 and Table 3.1.1 for the geometric orientation of the planar frame and the corresponding steel section assignments. A few additions are made to this frame system. The planar frames are placed at 20’ intervals and are connected at each frame joint with W12 x 16 girders. The resulting three – dimensional, steel – moment framed structure is shown in Figure 4.1.1. It should be noted that the frames at either end of the structure contain a different column orientation. To provide longitudinal stiffness, the columns are rotated 90 degrees so as to contribute their strong axis flexural properties in this direction.

Figure 4.1.1 Three-Dimensional Steel-Moment Frame Orientation

Three hazard – independent damage scenarios are proposed for application to the three – dimensional steel – moment frame system. The scenarios for this chapter are extrapolated from the damage scenarios defined in Chapter 3. It was seen that the all-2nd-floor-column case posed a significant threat to the stability of the planar frame. A similar investigation is proposed for the three – dimensional structure. The related damage scenario is the application of damage to all 1st floor columns. The 1st floor is chosen due to the increased complexity of the system. It is also hypothesized that the stiffer members associated with the 1st floor framing system may help to negate the effects of the all-floor-column type damage. Once again, an example of an event causing this type of damage could be related to seismic mode activation. In the previous chapter, the exterior 2nd floor column was a damage scenario investigated. The three – dimensional damage scenario extrapolated from this event damages the framing members along the longitudinal exterior face of the structure. This type of damage could be caused by an exterior blast, concentrated wind pressure, or a wind driven projectile. Lastly, the previous chapter investigated a scenario that damaged the 2nd floor interior column. The extrapolated three – dimensional damage scenario corresponding to this is defined by a concentrated central damage event that gradually moves outward. An example of such an event could be an interior blast. While examples of the possible events causing the proposed damage are given, it is vital to recall

the focus of this study is hazard – independent damage, and many other damage scenarios could be hypothesized.

Several figures are constructed to provide clarity of the proposed damage events. First, the all-1st-floor-columns damage scenario may be seen in Figure 4.1.2. Similar to Chapter 3, the damage levels are simply increased from a value of 0%, to a value of 80%. Once again, the 100% damage scenario is not investigated, as this scenario would lead to collapse.

Figure 4.1.2 All 1st Floor Columns Damage Scenario

Next, Figure 4.1.3 details the application of damage for the exterior longitudinal face case. As opposed to exact damage values, this scenario is defined by damage intensity levels. Damage Intensity Level 1 corresponds to the least amount of damage, while Damage Intensity Level 5 corresponds to the maximum amount of damage. The application of damage begins at the central frame, and then expands outward to the surrounding members. The color codes highlighted on the frame members correspond to a percent damage imposed to that particular member. Black, brown, orange, and red correspond to damage levels of 20%, 40%, 60%, and 80%, respectively. The indicators "A – E" define the damage intensity levels beginning with

Damage Intensity Level 1, and ending at Damage Intensity Level 5. It should be noted that only the frame members lying in the plane of the exterior longitudinal face are damaged. Members lying outside of this plane remain in their virgin condition.

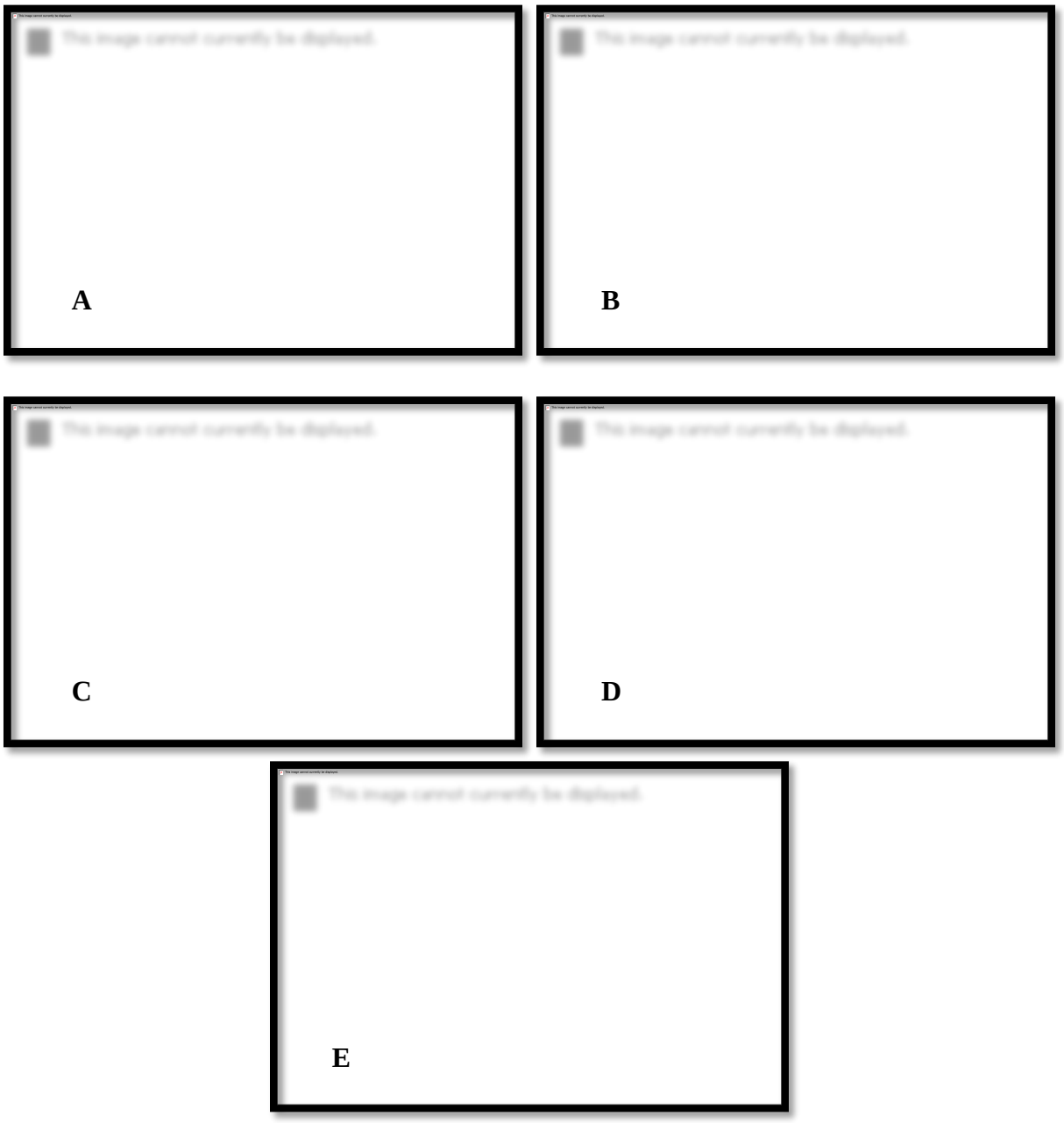

Figure 4.1.3 Longitudinal Exterior Face Damage Intensity Levels 1 – 5

The last damage scenario investigated, the concentrated interior damage, is displayed in Figure 4.1.4. This damage scenario is also described using the damage intensity level scheme. The damage begins at the central interior column, and expands outward as the damage intensity is increased. Once again, Damage Intensity Level 1 corresponds to the least damage, while Damage Intensity Level 2 corresponds to the maximum amount of damage. An identical color scheme is utilized to define the damage value imposed to each member. Black, brown, orange, and red correspond to damage values of 20%, 40%, 60%, and 80% respectively. As a final note, it should be recalled that the hazard – independent damage is applied as a reduction in the modulus of elasticity of the member receiving damage. The indicators "A – E" define the damage intensity levels beginning with Damage Intensity Level 1, and ending at Damage Intensity Level 5.

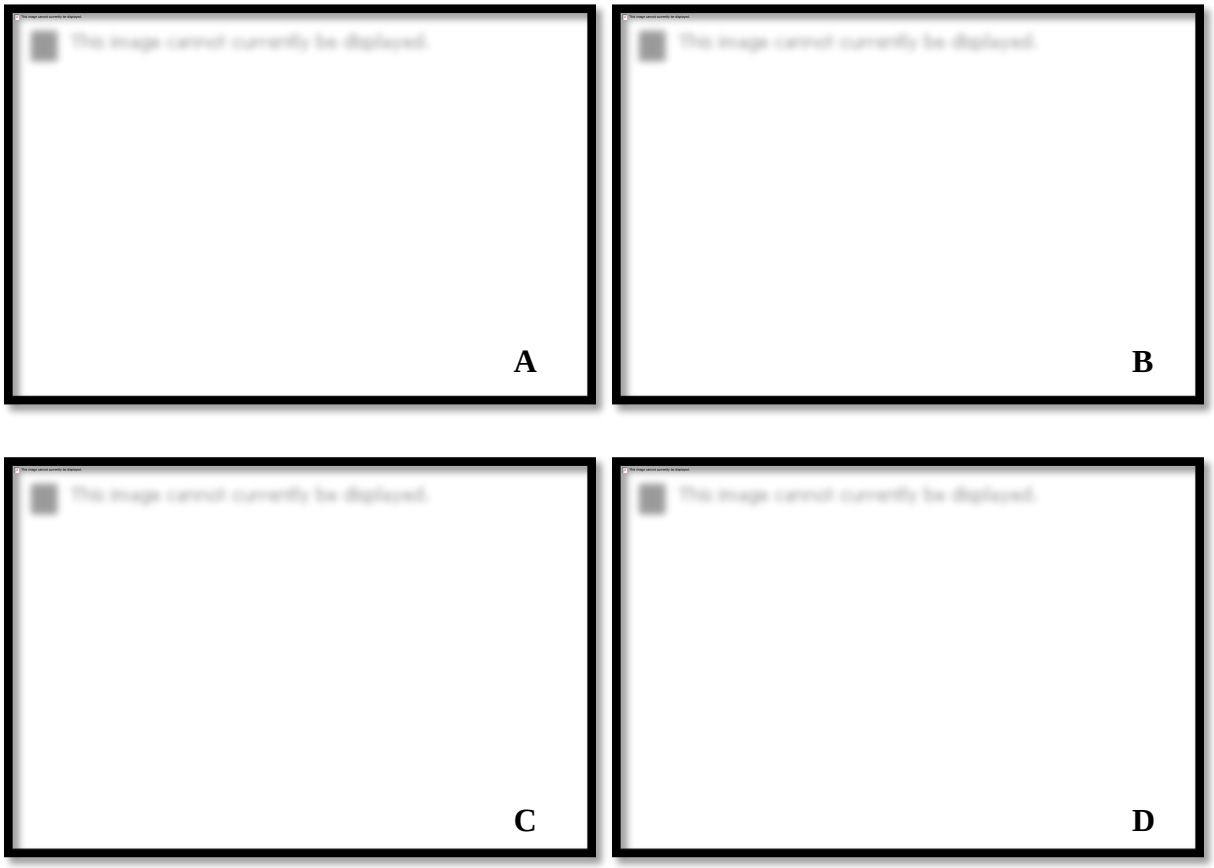

Figure 4.1.4 Concentrated Interior Damage Intensity Levels 1 – 5

Figure 4.1.4 Concentrated Interior Damage Intensity Levels 1 – 5

The load case applied to the three – dimensional, steel – moment frame structure is very similar to the case defined in Chapter 3. A difference arises only in the frames located at either end of the structure. Because their tributary areas are exactly half of the interior frame tributary areas, the forces applied to the end frames are simply divided by a factor of 2. Please refer to Tables 3.1.2 through 3.1.6 for the development of the applied loadings. Also, please refer to Figure 3.1.1 for an illustration of the location of the applied loading on the frame system. Once again, it is important to note that the values seen in these tables should be divided by a factor of 2 for the frames located at either end of the structure. It should be noted that the lateral load is applied perpendicular to the longitudinal face of the structure because the frame system being analyzed is not properly braced for lateral loading applied perpendicular to the transverse face of the structure.

Identical steps to those found in Chapter 3 are performed in ABAQUS/CAE for the application of the loads. First, the gravity loads are applied. This load is linearly increased from a value of 0, to its maximum value. Next, the lateral loads are applied. The lateral load is also linearly increased from a value of 0 to its maximum value. Second – order geometric effects are once again accounted for using the pre-defined function in the finite element software.

As a final step in the model development for Chapter 4, a note concerning plasticity should be made. Again, the application of the hazard – independent damage implies that a form of plasticity has been introduced into the system. For this reason, the plasticity checks performed in Chapter 2 are not continued in this chapter. Rather, an interaction capacity check is performed to ensure that the frame is adequately designed to resist the applied loading. Because both the loading and frame system are identical to that seen in Chapter 3, the "worst case" column is again the 1st floor interior column located in the central frame. For this reason, the calculation and result is identical to that which is displayed in Table 3.1.7. A reserve capacity of approximately 40% may be noted. This result implies that the applied loading suggested in the previous paragraphs does not pose a significant threat to the strength of the frame system. The following sections provide the results of the stability analyses performed for each hazard – independent damage scenario.

4.2 Stability Sensitivity: Hazard-Independent Damage of All 1st Floor Columns

In this section of Chapter 4, the hazard – independent damage application to all columns of the 1st floor and its effects on the stability of the three – dimensional, steel – moment frame are investigated. For the development of the steel frame model, applied loads, and damage scenarios, please refer to Section 4.1.

Several damage levels to the 1st floor columns are investigated to gain a broader understanding of the system's sensitivity to the damage scenario. The values of applied damage are 0%, 20%, 40%, 60%, and 80%. Again it should be noted that the damage is now applied through a reduction in the modulus of elasticity, and therefore it effectively reduces the stiffness of all degrees of freedom associated with a particular frame element. Identical load cases are analyzed for each damage level. That is, the only variable changing in the analyses performed is the level of the hazard – independent damage.

As detailed in Chapter 3, the inter-story drift of the affected floor and the total drift of the 4th floor are of primary interest. The lateral load corresponding to these locations is also tracked throughout the application of the loading. For this chapter, the inter-story drift is obtained for the 1st floor. Again, the inter-story drift is normalized by the column height, while the total drift is normalized by the full frame height. The lateral loads are normalized by the cumulative shear force at the respective floor level. That is, the 1st floor lateral load is normalized by the maximum applied shear force at the 1st floor, while the 4th floor lateral load is normalized by the total base shear. The results of the lateral displacements of the 1st floor and 4th floors after the application of the damage to all 1st floor columns are provided in Figure 4.2.1. The deformed configurations are also provided at a scale factor of 20.

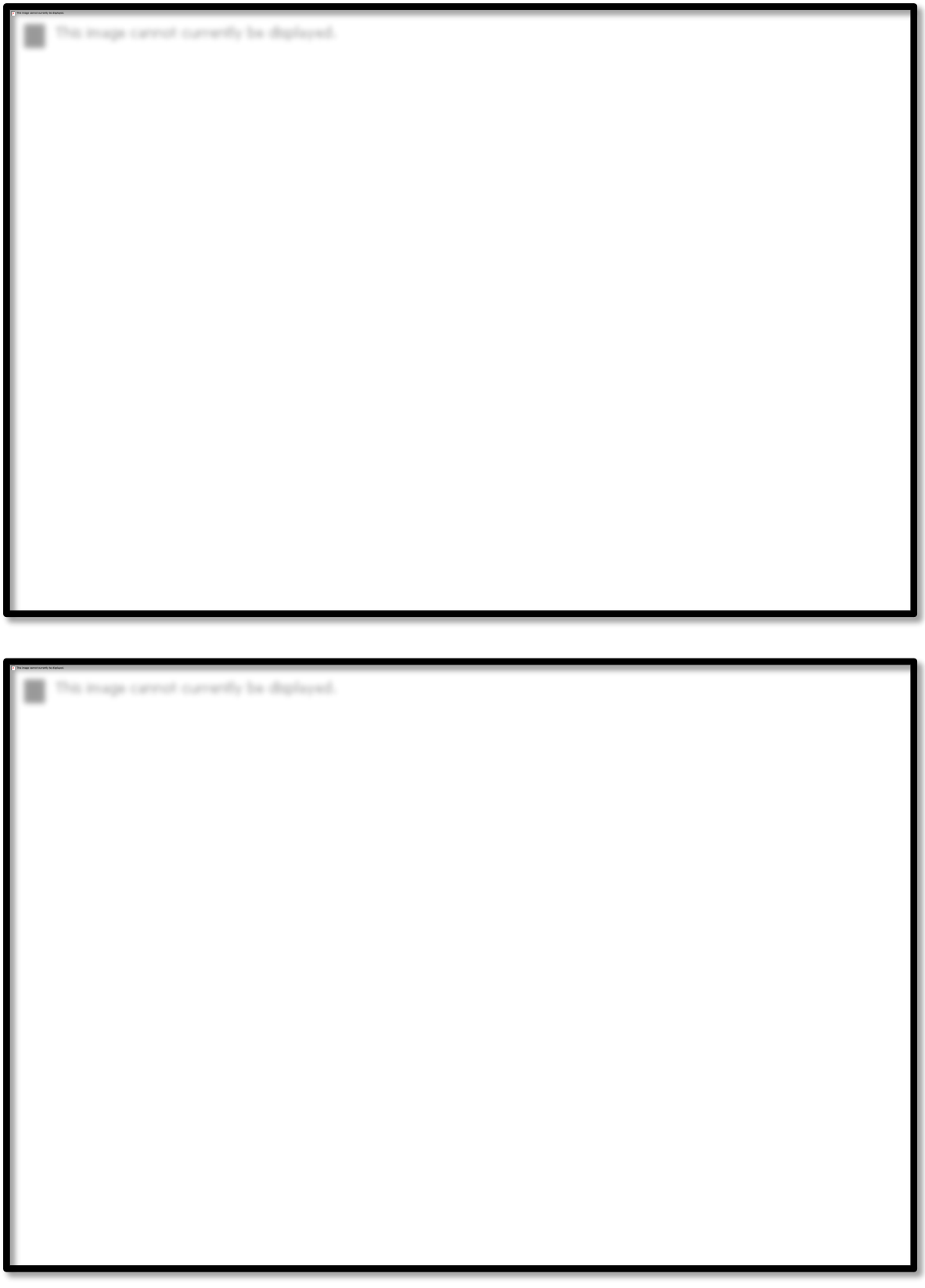

Figure 4.2.1(A) Inter-Story Drift of 1st Floor (B) Total Drift of 4th Floor

Attention is first directed to the inter-story drift of the 1st floor, as shown in Figure 4.2.1 (A). As expected, this damage scenario has a rather large impact as on the stability of the frame system. An inter-story drift of 1% of the column height is achieved below the maximum lateral load application for 80% damage case. The lateral load only reaches a value of approximately 90% of the cumulative shear. A 300% increase in the 1st floor inter-story drift is seen between the virgin state and the 80% damage level. This result, along with the exponential increase in the inter-story drift values between the different damage levels, indicates that the three – dimensional frame structure is sensitive to this damage scenario. A similar response may be seen by the total drift shown in Figure 4.2.1 (B). The 80% damage level results in a total drift of approximately 0.55% of the total frame height. This value is an increase of about 85% with respect to the virgin condition. While this effect is not as large as the inter-story drift effect, a definite threat to the stability of the structure may be seen.

Similar to Chapter 3, the changes in the slope, or stiffness, of the inter-story drift and total drift responses as a result of the damage scenario is investigated. Figure 4.2.2 illustrates the loss of stiffness versus the percent damage applied to all columns of the 1st floor for both the inter-story and total drift cases. Once again, damage is applied through a reduction of the modulus of elasticity of the member receiving damage. The load case applied to the frame system continues to remain unchanged from that defined in Section 4.1.

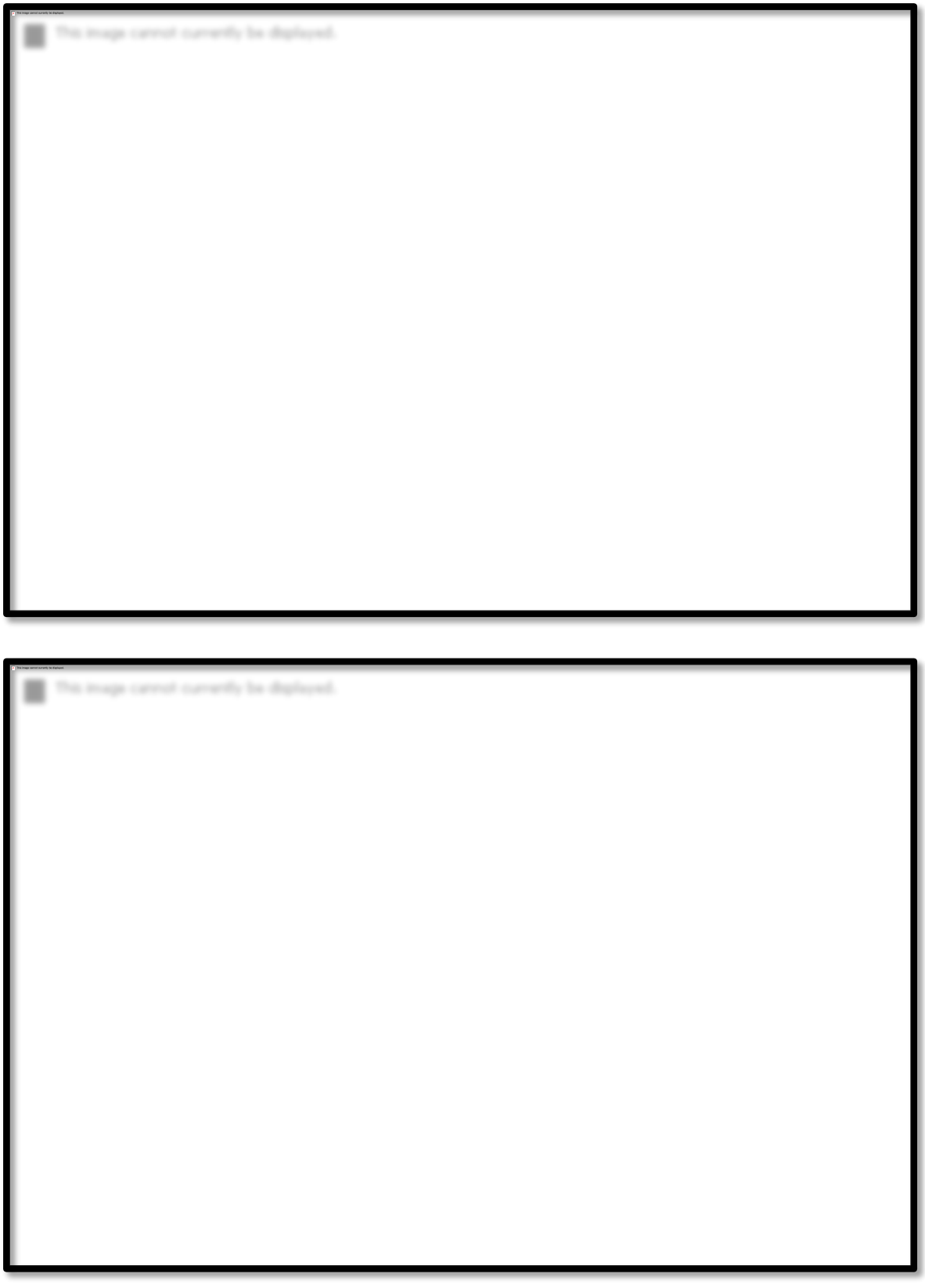

Figure 4.2.2 Loss of Stiffness vs. Percent Damage (A) 1st Floor (B) Global

Upon investigating Figure 4.2.2, several conclusions may be drawn. Both curves display highly nonlinear behavior. For this reason, it may be determined that any damage to the 1st floor column could result in potential stability issues. The loss of stiffness of the 1st floor with the application of damage is quite large, and a stable trend is not seen. A similar result may be seen for the global stiffness. The damage to all 1st floor columns leads to a potential stability issue for the total drift as well. A rapid loss of stiffness may be seen at the critical damage value of approximately 65%. That is, at this damage level, the structure begins to rapidly approach instability. It should be noted that results of this section are not dependent on the direction of the loading, so long as it remains perpendicular to the longitudinal face. The symmetry of the applied damage provides this property. Through the results displayed in this section, it may be determined that the three – dimensional frame structure is sensitive to the all-1st-floor-columns damage scenario.

4.3 Stability Sensitivity: Hazard-Independent Damage of Longitudinal Exterior Face

In this section of Chapter 4, the hazard – independent damage application to the longitudinal exterior face and its effects on the stability of the three – dimensional frame system are investigated. For the development of the steel frame model, applied loads, and damage scenarios, please refer to Section 4.1.

Several damage levels are imparted to the exterior longitudinal face of the three – dimensional frame system. As previously discussed, these values are now described as damage intensity levels. Damage Intensity Level 1 imparts the least amount of damage, while Damage Intensity Level 5 imparts the maximum amount of damage. To view the development of the different damage levels, please refer to Figure 4.1.3.

The inter-story drift of the 1st floor and the total drift of the 4th floor remain the primary variables investigated throughout the analyses. The development of the lateral load applied to these floors also remains an important variable in the study. Both the story drifts and lateral loads are normalized using the same techniques defined in Section 4.2. It should be noted that the 1st floor inter-story drift is chosen simply as a common reference for all three damage scenarios. The results of the lateral displacements of the 1st and 4th floors after the application of damage to the exterior longitudinal face are provided in Figure 4.3.1. The deformed configurations are also provided at a scale factor of 20.

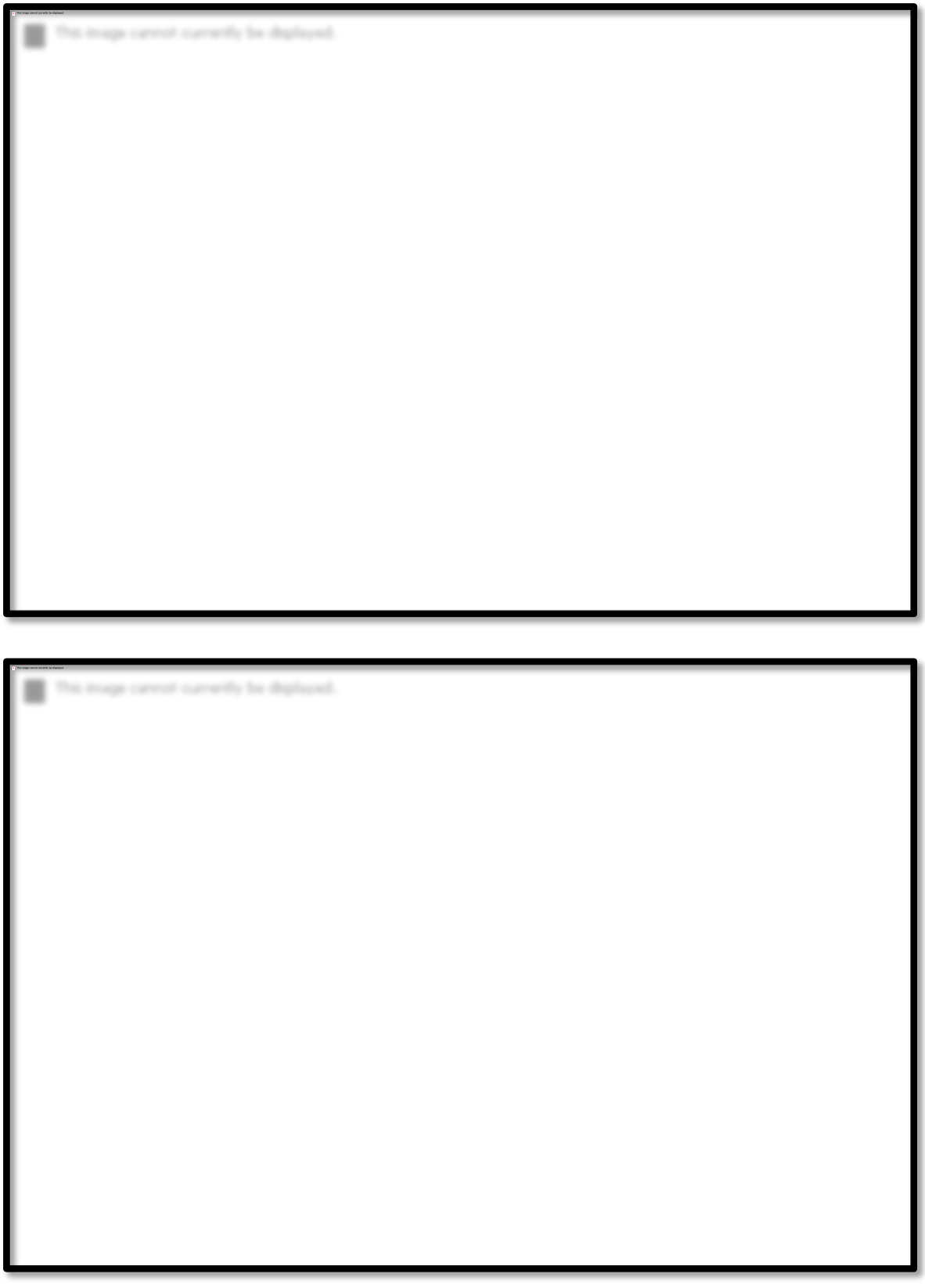

Figure 4.3.1 (A) Inter-Story Drift of 1st Floor (B) Total Drift of 4th Floor

The results of the damage effect on the inter-story drift, as shown in Figure 4.3.1 (A), are investigated first. A relatively minimal effect on the 1st floor inter-story drift is seen as a result of damaging the longitudinal exterior face. The maximum damage case, Damage Intensity Level 5, yields a drift value of approximately 0.35% of the column height. This is approximately a 40% increase from the virgin condition. While this is a significant increase, the resulting inter-story drift value is relatively low. It may be inferred that the three – dimensional, steel – moment frame structure is not highly sensitive to this damage scenario.

Next, the results of the damage effect on the total drift of the 4th floor, as shown in Figure 4.3.1 (B), are investigated. Once again only a small increase in the total drift values may be seen in this damage scenario. Damage Intensity Level 5 results in a total drift value of approximately 0.35% of the total frame height. This value is only a 15% increase from the virgin state. The effect of this damage scenario on the story drifts is certainly not profound.

The changes in the slope, or stiffness, of the inter-story drift and total drift responses as a result of the damage is again analyzed. Figure 4.3.2 illustrates the loss of stiffness versus the damage intensity level for both the inter-story and total drift cases.

Figure 4.3.2 Loss of Stiffness vs. Percent Damage (A) 1st Floor (B) Global

As expected, only a small effect on the 1st floor and global stiffnesses may be seen in Figure 4.3.2. The highest damage intensity, Damage Intensity Level 5, produces a loss of the 1st floor stiffness of approximately 20%. It should also be noted that no significant increase in the loss of the 1st floor stiffness is seen from Damage Intensity Level 4 and Damage Intensity Level 5. Figure 4.3.2 (B) illustrates a similar trend for the global stiffness. A minor loss of only 8% of the global stiffness is seen at Damage Intensity Level 5. These results suggest that the three – dimensional, steel – moment frame structure is not particularly sensitive to this damage scenario. It should be noted however, that this result is largely dependent on the direction of the lateral load. A lateral load applied in the opposite direction would likely produce a much more devastating effect on the stability of the system.

4.4 Stability Sensitivity: Hazard-Independent Damage of Central Interior Members

In the final section of Chapter 4, the hazard – independent damage application to the central interior frame members and their effect on the stability of the three – dimensional, steel – moment frame are investigated. For the development of the steel frame model, applied loads, and damage scenarios, please refer to Section 4.1.

Once again, the damage intensity level scheme is utilized to describe the amount of damage introduced into the system. The Damage Intensity Level 1 refers to the least amount of damage, while the Damage Intensity Level 5 refers to the maximum amount of damage. The reduction of the modulus of elasticity of the member receiving damage effectively applies the damage associated with the concentrated central damage scenario. The load case applied to the frame system continues to remain unchanged from that defined in Section 4.1.

The inter-story drift of the 1st floor and the total drift of the 4th floor remain the primary variables investigated throughout the analyses. The development of the lateral load applied to these floors also remains an important variable in the study. Both the story drifts and the lateral loads are normalized using the same techniques defined in Section 4.2. The results of the lateral displacements of the 1st and 4th floors after the application of damage to all of the 2nd floor columns are provided in Figure 4.4.1. The deformed configurations are also provided at a scale factor of 20.

Figure 4.4.1 (A) Inter-Story Drift of 1st Floor (B) Total Drift of 4th Floor

The results of the damage effect on the inter-story drift, as shown in Figure 4.4.1 (A), are investigated first. The three – dimensional frame system illustrates a significant change in response with the introduction of the concentrated, centralized damage scenario. The Damage Intensity Levels 4 and 5 both result in 1st floor inter-story drift values of 1% of the column height. Only 50% of the cumulative shear is achieved before reaching the drift limit for Damage Intensity Level 5. Approximately a 300% percent increase in the inter-story drift is seen between the virgin state and Damage Level 5. Exponential increases in the 1st floor inter-story drift may be seen between the different damage intensity levels.

Next, the results of the damage effect on the total drift of the 4th floor, as shown in Figure 4.3.1 (B), are investigated. Again, a rather large effect on the response of the frame system may be noted. A total drift value of 1% of the total height of the frame is obtained at approximately 72% of the total base shear for Damage Intensity Level 5. It should be noted that this magnitude of lateral displacement would likely be devastating for the frame system and collapse is probable. A 230% increase in the total drift value is seen between the virgin state and Damage Intensity Level 5. Again, an exponential increase in the total drift values may be seen between the damage intensity levels.

The changes in the slope, or stiffness, of the inter-story drift and total drift responses as a result of the damage is once again analyzed. Figure 4.4.2 illustrates the loss of stiffness versus the damage intensity level for both the inter-story and total drift cases.

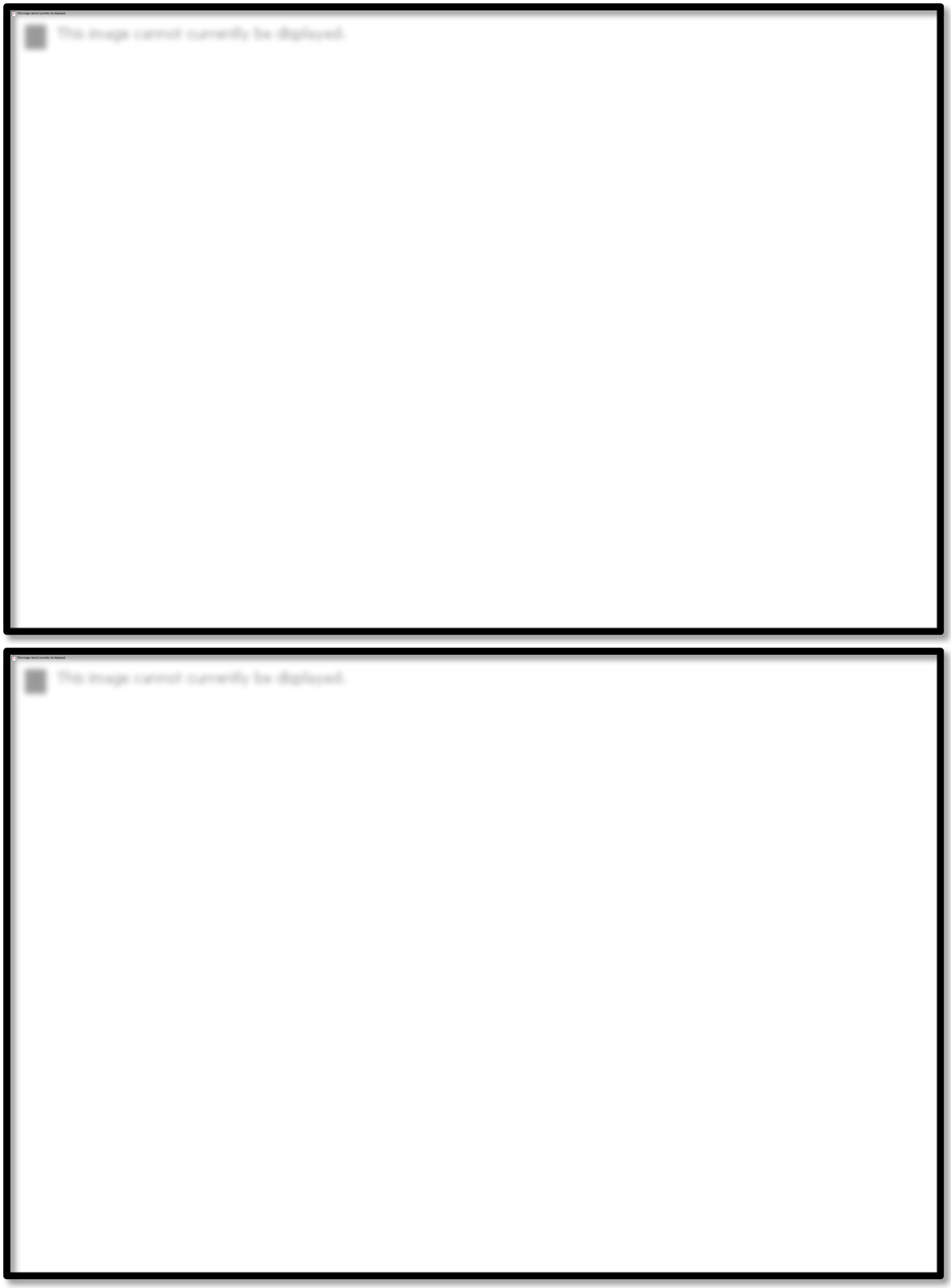

Figure 4.4.2 Loss of Stiffness vs. Percent Damage (A) 1st Floor (B) Global

Upon examining the results of Figure 4.4.2, several conclusions may be drawn. Both curves are highly unstable and nonlinear in nature. This illustrates a rather large effect of this particular damage scenario on the stability of the frame system. The 1st floor and global stiffness loss curves both change slopes several times. It is possible that this effect is a result of the alternate load paths of the three – dimensional frame system being activated. Despite the alternate load paths, the response of the frame system is highly unstable. A damage scenario similar to that investigated in this section would have devastating effects on the stability of the frame system. As a final note, it should be made known that the direction of the lateral load does not affect the results in this section. The symmetry of the applied damage provides this property. The following chapter contains several concluding remarks regarding the stability studies performed within this work, as well as recommendations for future work.

5. CONCLUSIONS AND RECOMMENDATIONS FOR FUTURE WORK

Chapter 5 provides concluding remarks regarding the analyses performed in the previous Chapters 2 through 4. Recommendations for future work are also made in this chapter.

Chapter 2 illustrates how second – order effects and damage may lead to the onset of instability. Limits for the axial load applied to beam – column elements that cause bifurcation of equilibrium and excite second – order geometric effects are calculated. These limits are known as elastic critical buckling loads. Results of the study indicate that damage reduces the elastic critical buckling load. Lastly, force versus deflection curves are obtained for a simple portal frame. The figures obtained aid in illustrating how second – order geometric effects and hazard – independent damage effect the system response and may lead to instability.

Chapter 3 investigates the stability of a 4 story – 2 bay planar steel frame subjected to three hazard – independent damage scenarios. It is found that damage scenarios involving damage to the interior column or all columns of the 2nd floor could lead to instability of the structure. That is, the frame investigated shows sensitivity to these damage scenarios under the loading conditions prescribed in Chapter 2.

Chapter 4 defines three additional hazard – independent damage scenarios that are applied to a three – dimensional extension of the planar frame found in Chapter 3. Sensitivity of the structure's stability is found in centralized interior and all 1st floor column damage scenarios. The results of this study are strictly controlled by the application of the lateral load. This loading is only applied perpendicularly to the longitudinal face of the frame, because the system is not

braced for loading perpendicular to the transverse face of the frame.

For future studies, several suggestions can be made. First, a wider range of lateral loading scenarios may be investigated in order to gain a broader understanding of their impact on the stability of the structure. However, in order to do so, a bracing system should be included in the three – dimensional frame system. This will provide a greater stiffness in its weak axis. Also, additional damage scenarios could be investigated. Because the damage is hazard – independent, there is virtually no limit to the hypothetical damage scenarios that may be investigated. Lastly, the frame elements in the computational model may be sub-divided in order to allow for a more refined distribution of damage. However, too much refinement may lead to a tedious modeling process. Diminishing returns would be expected at this point, because a hazard – dependent scenario would result in comparable computations, but with a much more accurate result.

In conclusion, the methods detailed in this work provide a robust method that allows stability investigations for a multitude of damage scenarios to be performed. However, careful consideration of the assumption and implications of this method should be taken before it is applied outside the scope of this research.

BIBLIOGRAPHY

ABAQUS Inc. (2003). *User's Manual.* Simulia.

American Institute of Steel Construction. (2011). *Steel Construction Manual.* United States: AISC.

American Society of Civil Engineers. (2005). *Minimum Design Loads for Buildings and Other Structures.* Danvers: American Society of Civil Engineers.

Balling, R., & Lyon, J. (2011). Second-Order Analysis of Plane Frames with One Element Per Member. *Journal of Structural Engineering*, 137(11) 1350 - 1358.

Belytschko, T., Liu, W. K., Moran, B., & Elkhodary, K. (2014). *Nonlinear Finite Elements for Coninua and Strucutres.* Singapore: John Wiley & Sons.

Bruneau, M., Uang, C.-M., & Sabelli, R. (2011). *Ductile Design of Steel Structures.* New York: McGraw Hill.

Chen, W., & Lui, E. (1987). *Structural Stability Theory and Implementation.* New York: Prentice Hall.

Chen, W., & Lui, E. (1991). *Stability Design of Steel Frames.* Florida: CRC Press.

Cortes, G., Liu, J., & Francisco, T. (2015). Framing Strategies fr Robustness in Steel Buildings. *Structures Congress* (pp. 1118 - 1129). ASCE.

Galambos, T. (1998). *Guide to Stability Design Criteria for Metal Structures.* New York: John Wiley & Sons.

Geschwindner, L. F. (2008). *Unified Design of Steel Structures.* New Jersey: John Wiley & Sons, Inc.

Hughes, T. (1987). *The Finite Element Method.* Mineola: Dover Publications.

Li, G.-Q., & Li, J.-J. (2007). *Advanced Analysis and Design.* London: John Wiley & Sons.

Li, Y., Song, R., & Van De Lindt, J. (2014). Collapse Fragility of Steel Structures Subjected to

Earthquake Mainshock-Aftershock Sequences. *Journal of Strucutral Engineering*, 0401 4095 1 - 10.

MacRae, G., Kimura, Y., & Roeder, C. (2004). Effect of Column Stiffness on Braced Frame Seismic Behavior. *Journal of Structural Engineering*, 130(3) 381 - 391.

McGuire, W., Gallagher, R., & Ziemian, R. (2000). *Matrix Structural Analysis.* Digital Commons: Faculty Books.

Powell, G. (2010). *Modeling for Structural Analysis: Behavior and Basics.* China: Computers and Structures Inc.

Sezen, H., & Akah, E. (2015). Collapse Analysis and Testing of an Existing Building. *Strucutres Congress* (pp. 1078-1089). ASCE.

Timoshenko, S., & Gere, J. (1961). *Theory of Elastic Stability.* Mineola: Dover Publications.

Yang, Y.-B., & Kuo, S.-R. (1994). *Theory & Analysis of Nonlinear Framed Structures.* Singapore: Prentice Hall.

LIST OF APPENDICES

APPENDIX A: PINNED BASE PORTAL FRAME CALCULATIONS


This image cannot currently be displayed.


This image cannot currently be displayed.

APPENDIX B: FIXED BASE PORTAL FRAME CALCULATIONS

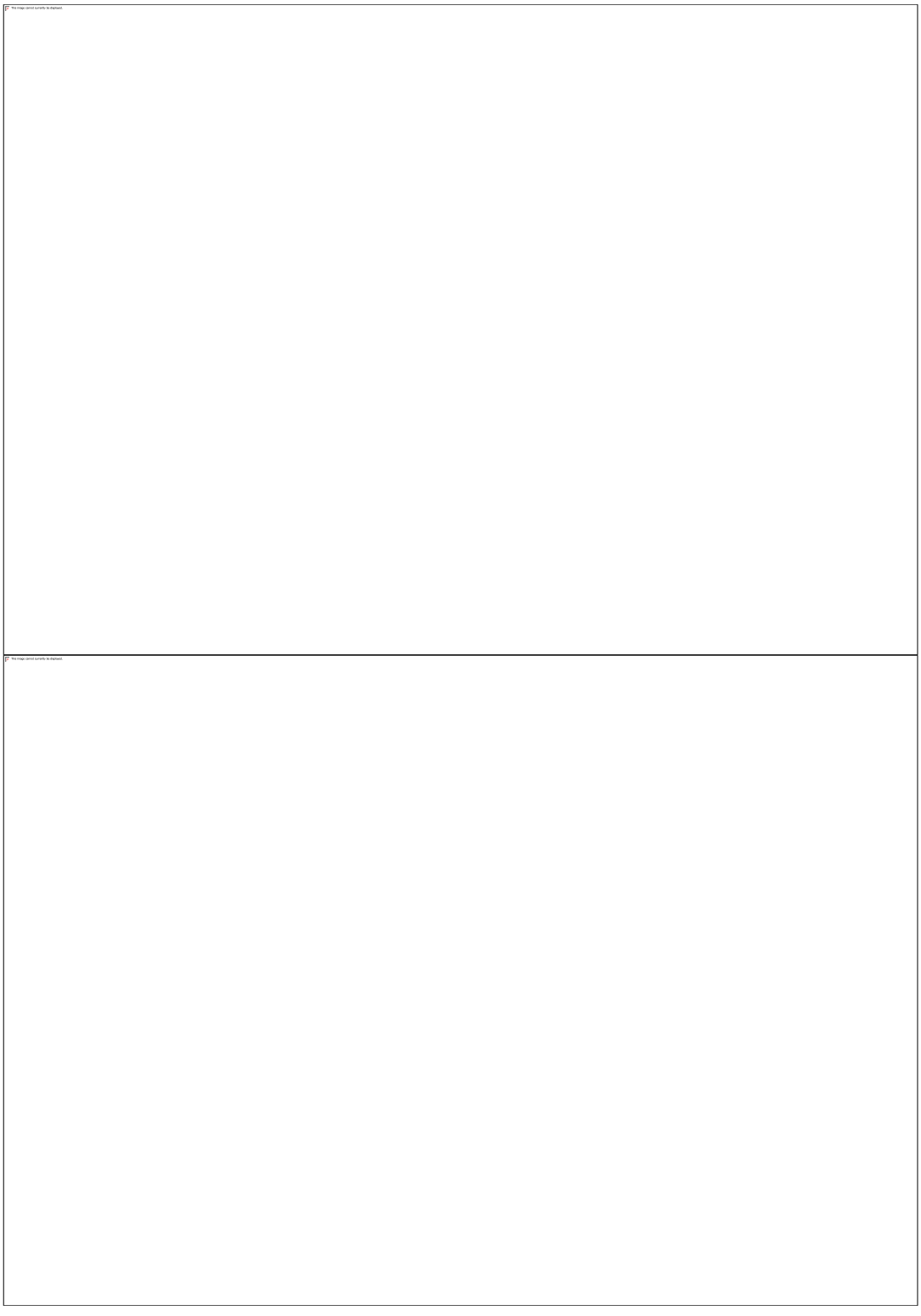

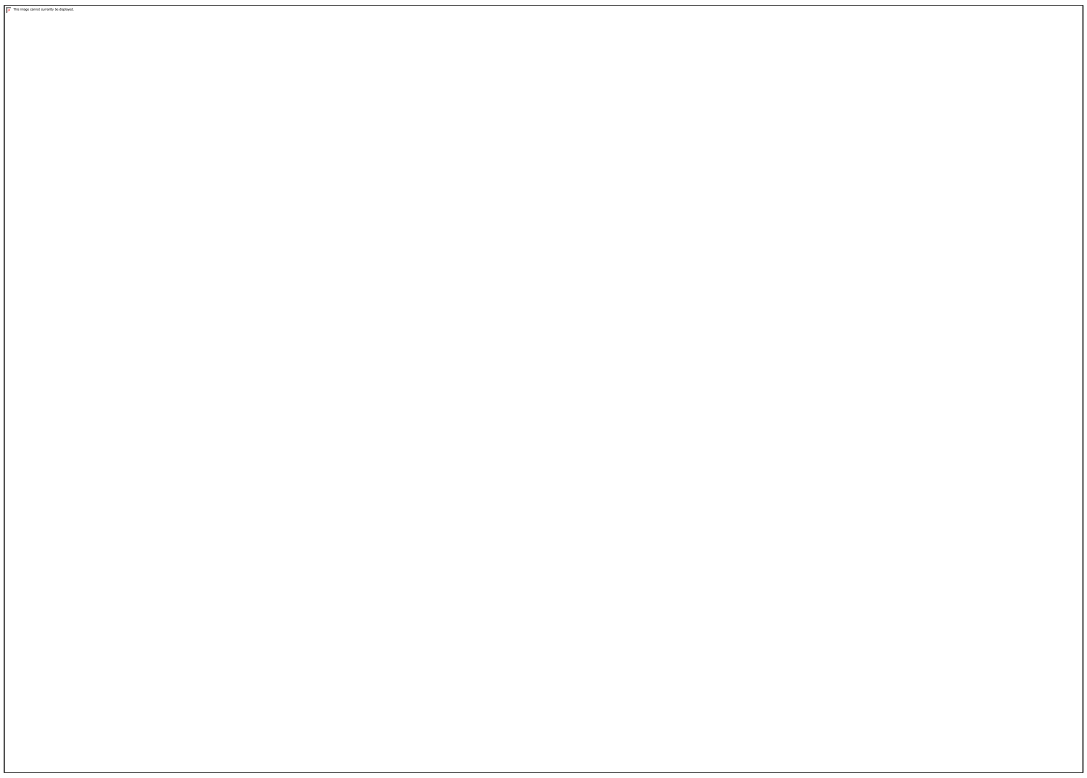

APPENDIX C: PLASTICITY CALCULATIONS

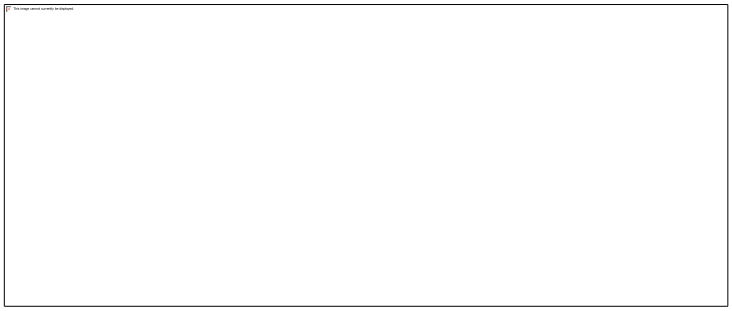

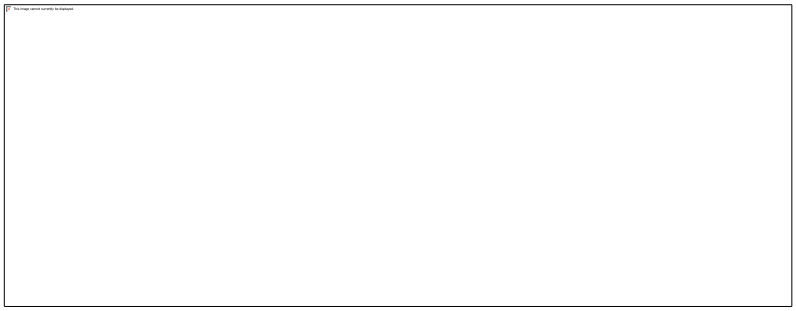

VITA

TREY POWELL, E.I.

1502 Abbeyville Street · Pascagoula, MS 39581 · (228) 623-8641 · trpowell@go.olemiss.edu

EDUCATION

M.S., Engineering Science, University of Mississippi, 2016
Thesis: Stability Sensitivity of Low-Rise Steel-Moment Framed Buildings to Hazard-Independent Damage
B.S., Civil Engineering, University of Mississippi, May 2014

TEACHING EXPERIENCE

Teaching Assistant, 2012-2016
University of Mississippi
Course: Statics, Structures Lab

Research Assistant, 2014-2016
University of Mississippi
Dr. Christopher Mullen, Civil Engineering, NCITEC/Columbia University Blast Study

INDUSTRY EXPERIENCE

Civil Engineering Student Intern, Summer 2013
Neel-Schaffer Inc.
Pascagoula, Mississippi

Structural Engineering Student Intern, Summer 2015
Thompson Engineering
Mobile, Alabama

HONORS AND FELLOWSHIPS

School of Engineering Class Marshall, 2014
Taylor Medal Recipient, 2014
Phi Kappa Phi Honor Society
Tau Beta Pi Honor Society
Chi Epsilon Honor Society
ASCE Ole Miss President, 2014
Graduate School Honors Fellowship